

Uncertainties of Ocean Wave Parameters Estimated from HF Radar Sea-Echo under Typhoon conditions

Hwa CHIEN

Duy-Toan DAO

Institute of Hydrological and Oceanic Sciences, National Central University, TAIWAN

Sep 13, 2018

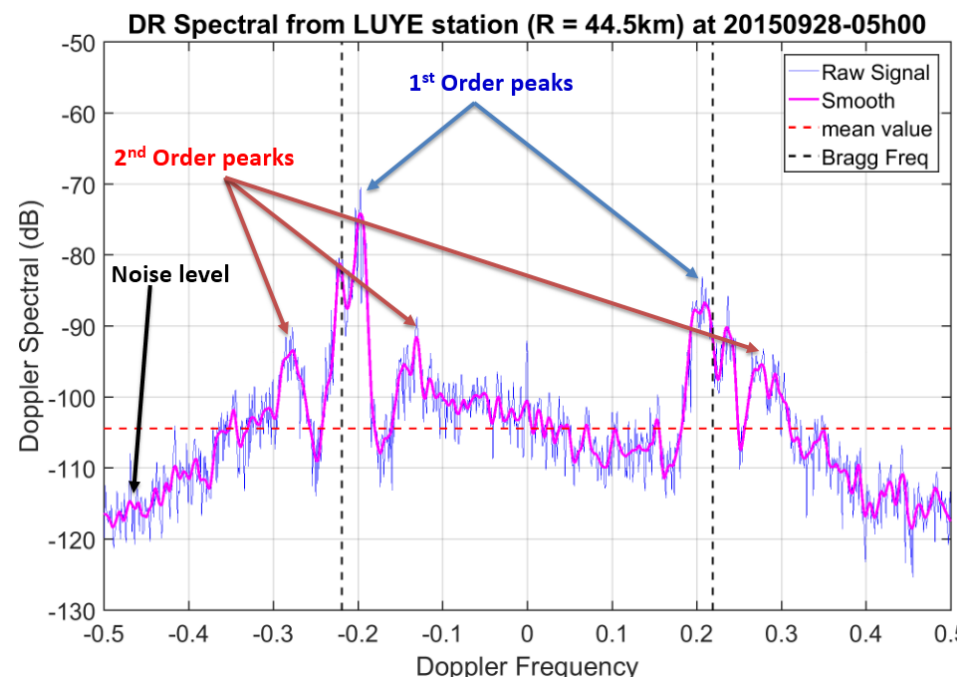
Theoretical Base: Barrick's Theory

- The First-Order Doppler spectrum, $\sigma^{(1)}(\omega)$

$$\sigma^{(1)}(\omega) = 2^6 \pi k_0^4 \sum_{m=\pm 1} S(-2m\mathbf{k}_0) \delta(\omega - m\omega_B) \quad (1)$$

- The Second-Order Doppler spectrum, $\sigma^{(2)}(\omega)$

$$\sigma^{(2)}(\omega) = 2^6 \pi k_0^4 \sum_{m_1, m_2 = \pm 1} \int_{-\infty}^{+\infty} \int_{-\infty}^{+\infty} |\Gamma|^2 S(m_1 \mathbf{k}_1) S(m_2 \mathbf{k}_2) \delta(\omega - m_1 \sqrt{gk_1} - m_2 \sqrt{gk_2}) dp dq \quad (2)$$



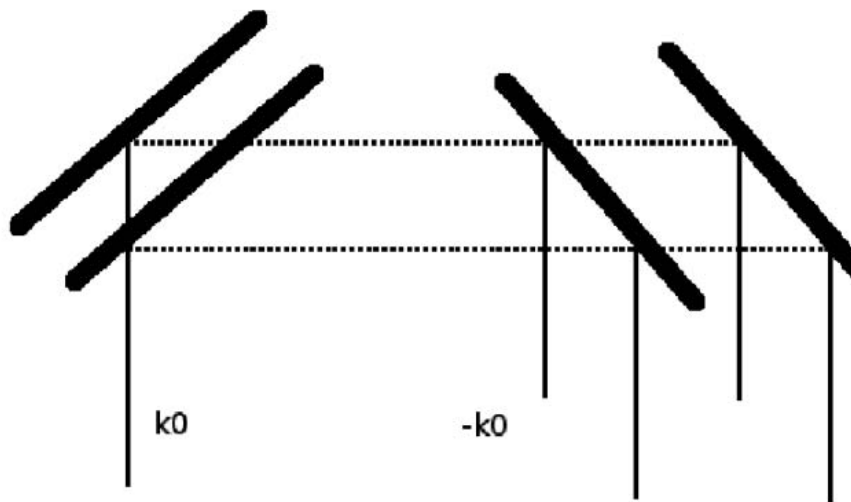
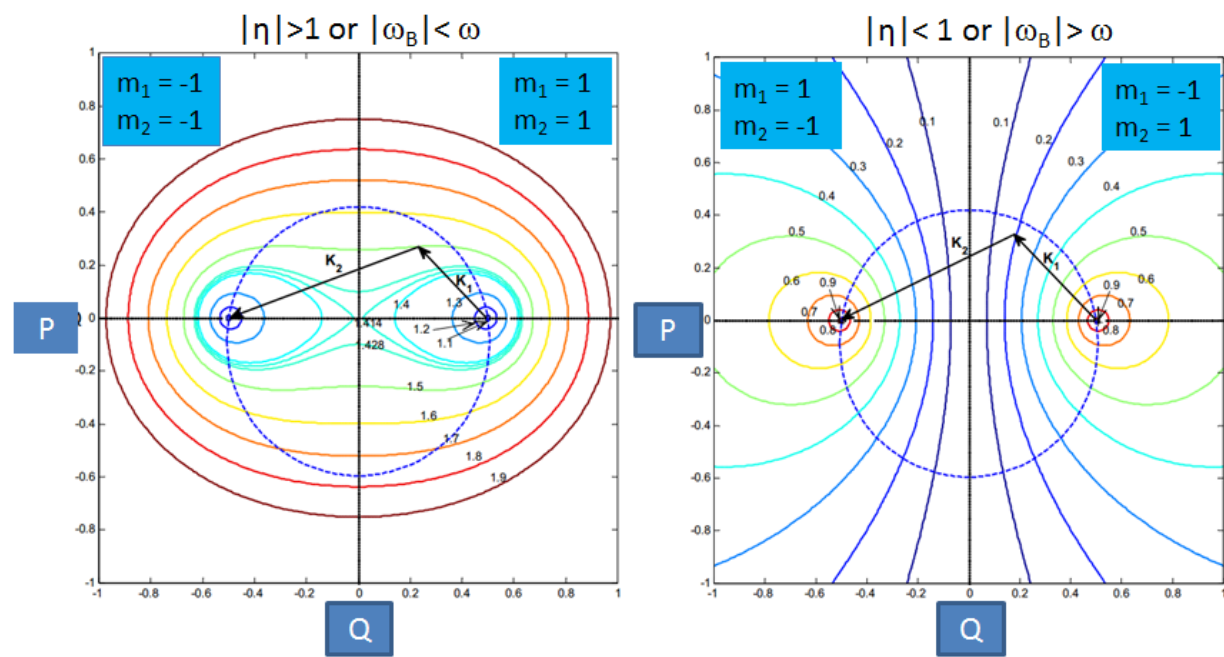
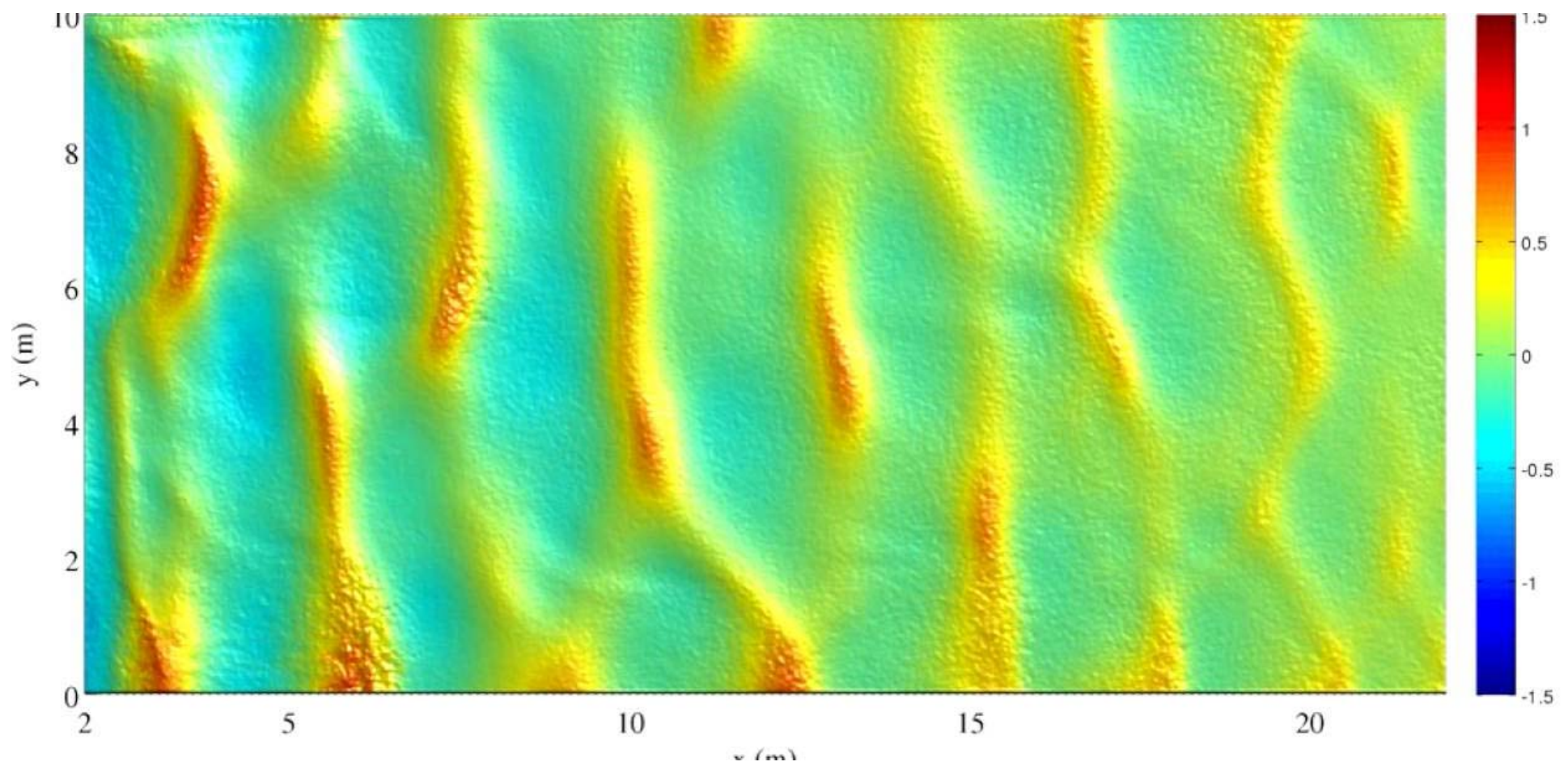
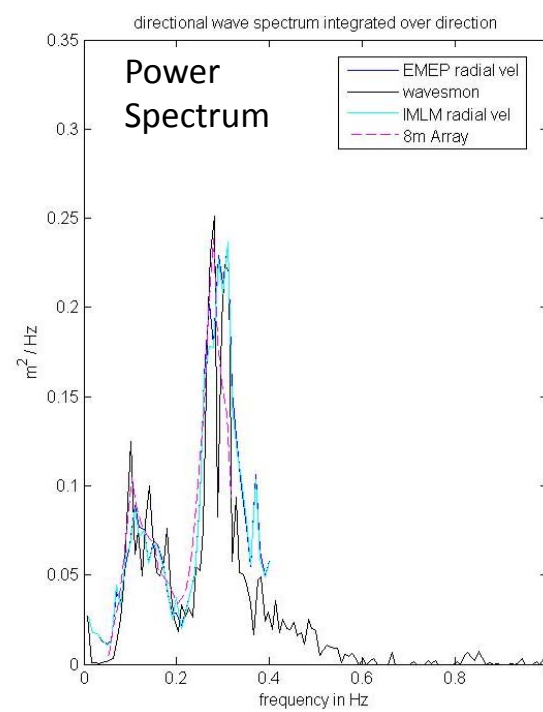
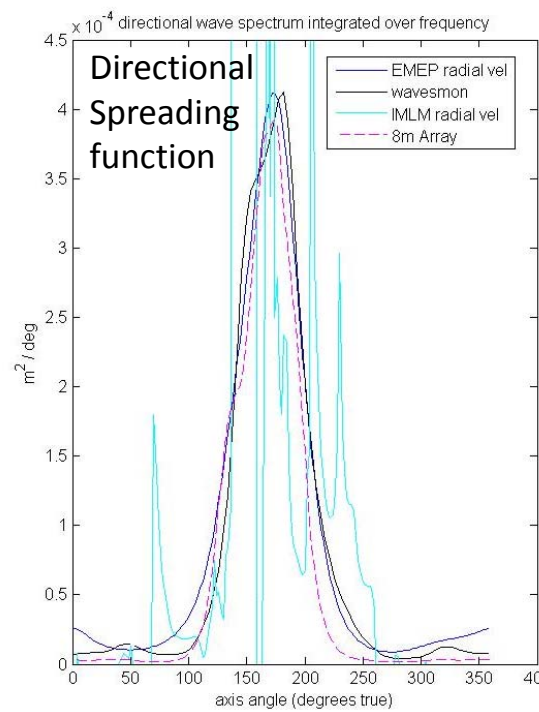
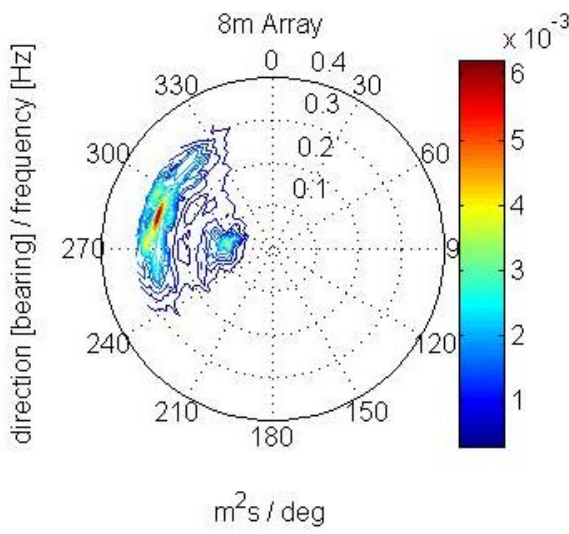
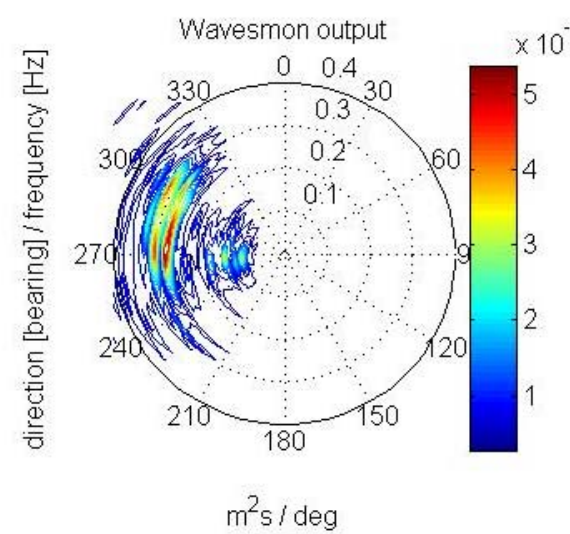
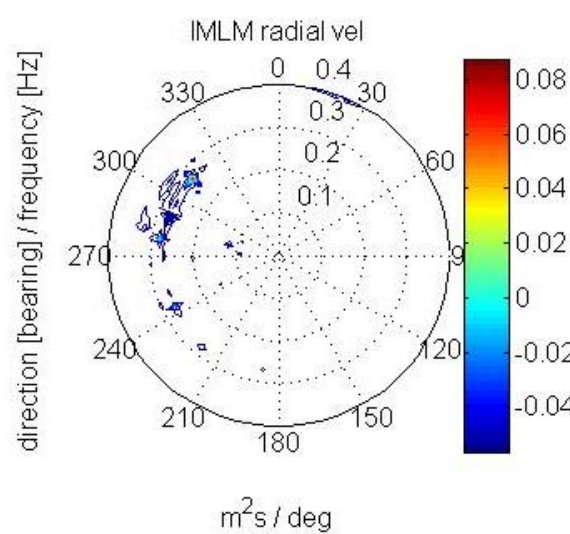
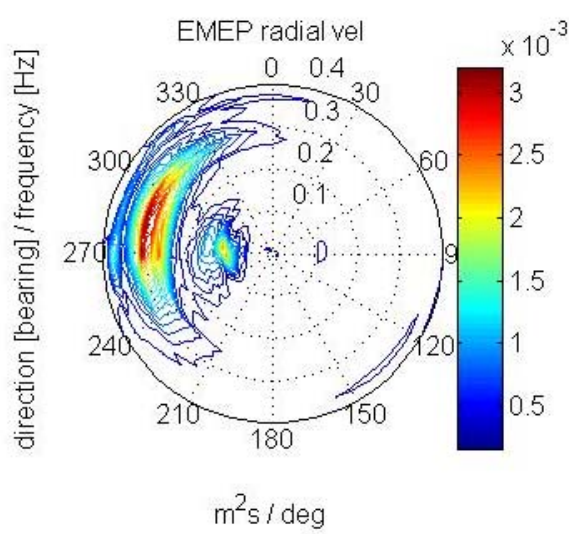


Figure 1.5: Electromagnetic double-scattering. The incident radar wavevector k_0 is on the left. Multiple coherent received wavevectors $-k_0$ are on the right.

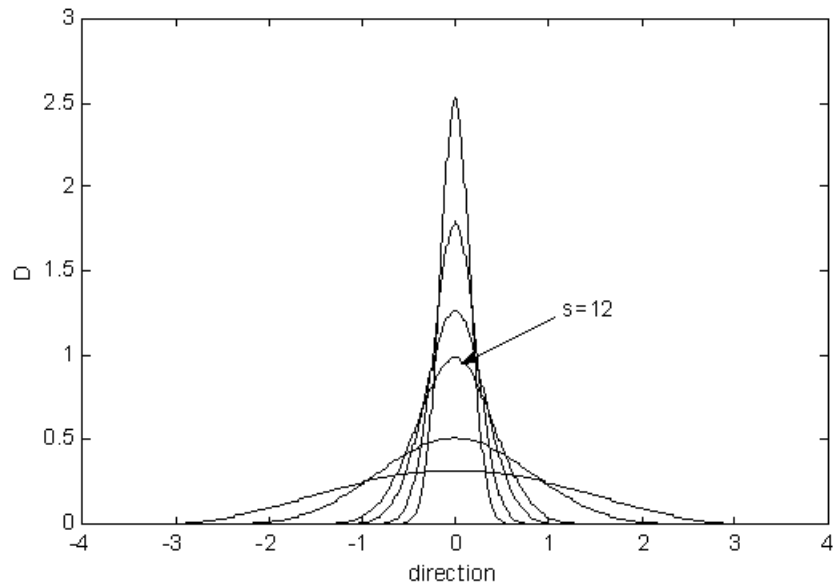
$$k_1 + k_2 = -2k_0$$







Wave Directional Spreading



$$G(\theta) = Q(s) \cos^{2s} \left\{ \frac{[\theta - \theta_m]}{2} \right\}$$

Mitsuyasu et al. (1975)

$$s = \begin{cases} s_0 (f / f_p)^5 & f \leq f_p \\ s_0 (f / f_p)^{-2.5} & f > f_p \end{cases}$$

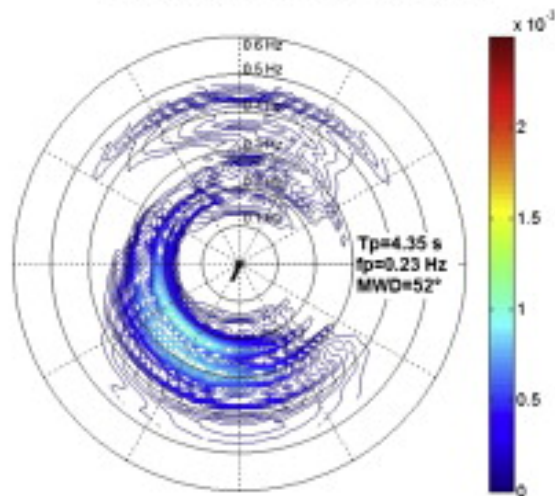
$$s_0 = 11.5 (2\pi f_p U / g)^{-2.5},$$

Goda (1985)

$$s_0 = \begin{cases} 10 & \text{wind waves,} \\ 25 & \text{Swell(short decay distance),} \\ 75 & \text{Swell(long decay distance).} \end{cases}$$

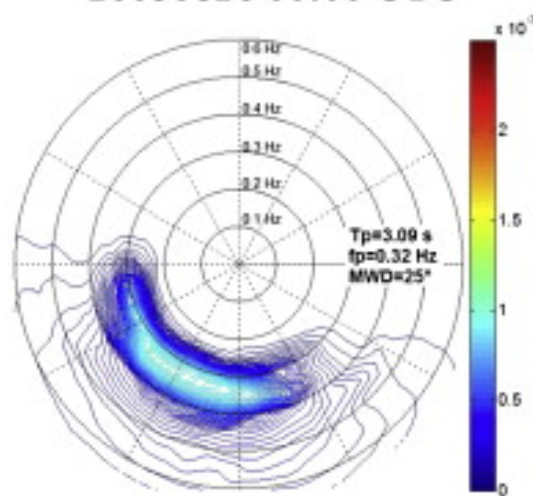
B

Buoy 42003
20050826 00:00 UTC



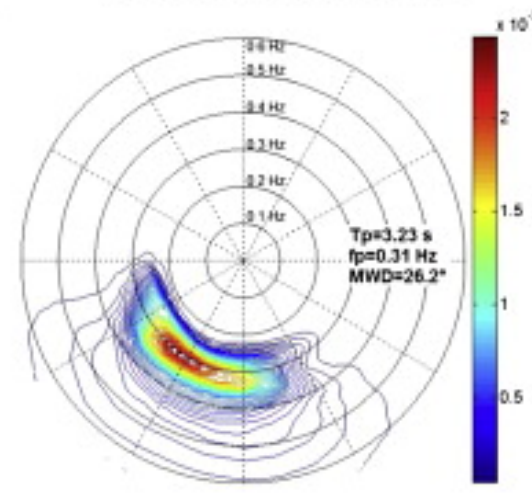
$H_s = 0.50 \text{ m}$; $WD = 23.0^\circ$, $WSPD = 6.5 \text{ m/s}$

SWAN
20050826 00:00 UTC

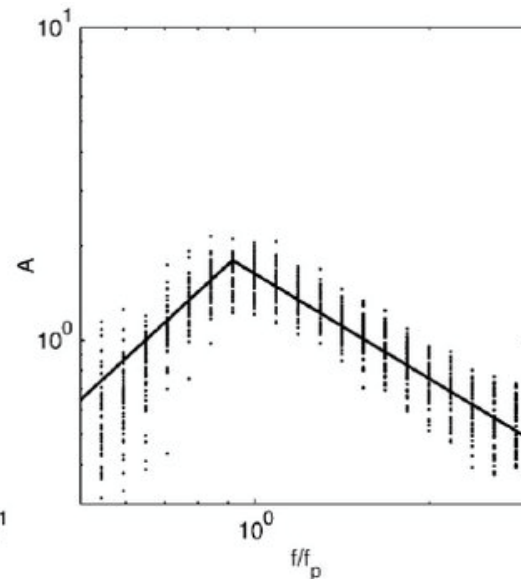
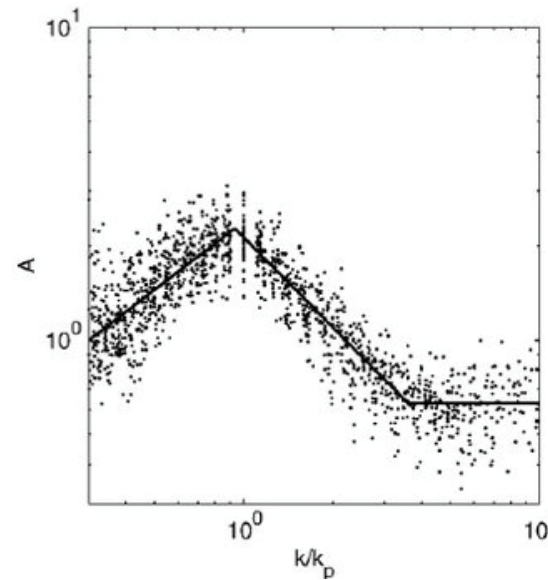
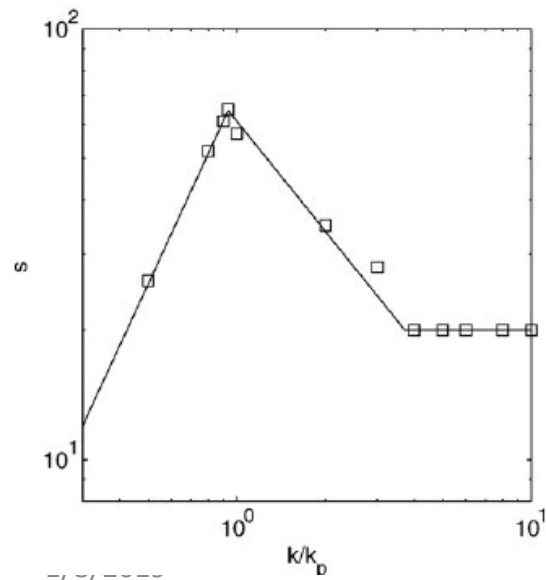


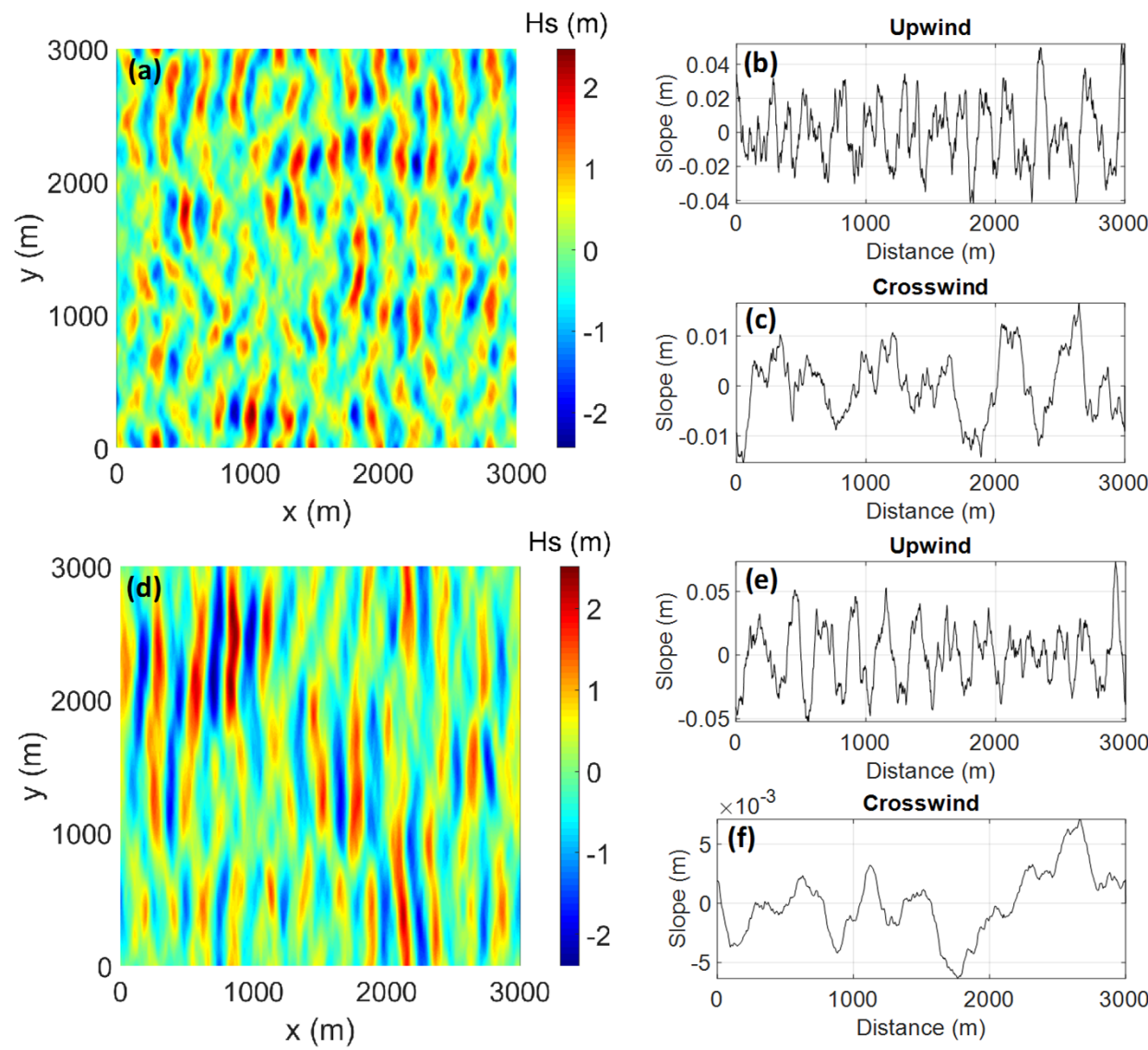
$H_s = 0.51 \text{ m}$; $WD = 16.7^\circ$, $WSPD = 6.5 \text{ m/s}$

WWIII
20050826 00:00 UTC

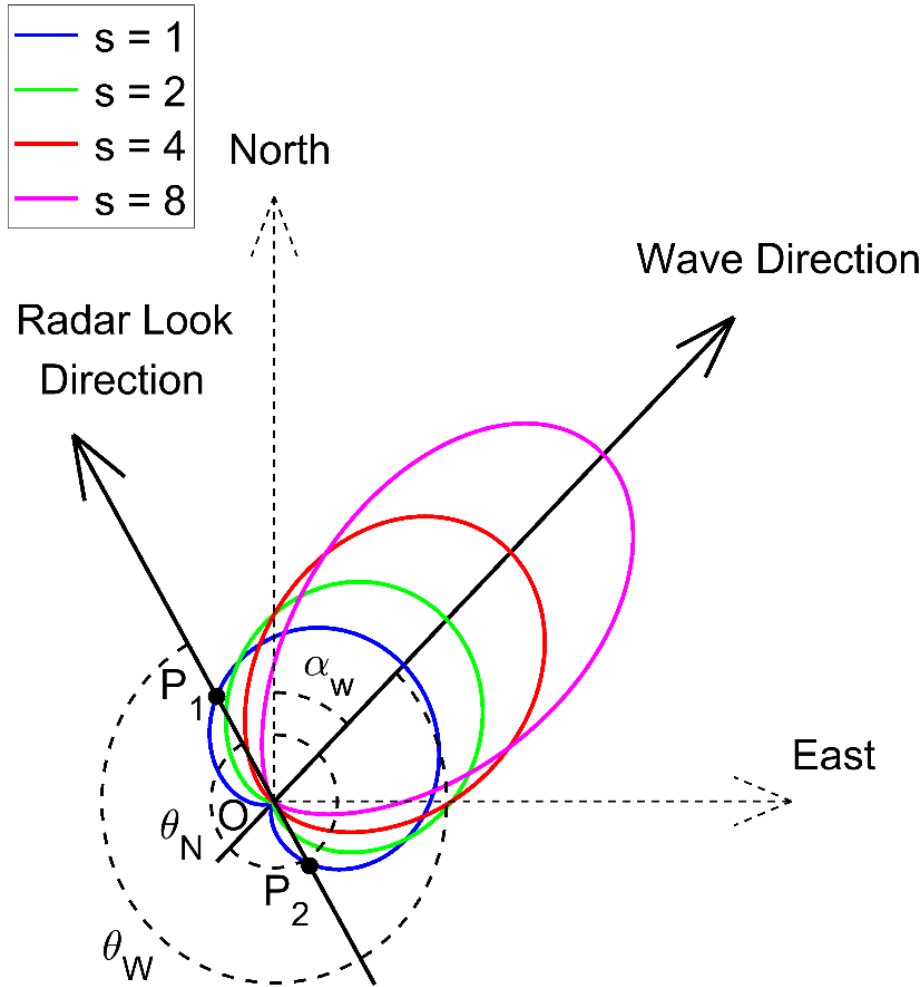


$H_s = 0.59 \text{ m}$; $WD = 16.7^\circ$, $WSPD = 6.5 \text{ m/s}$



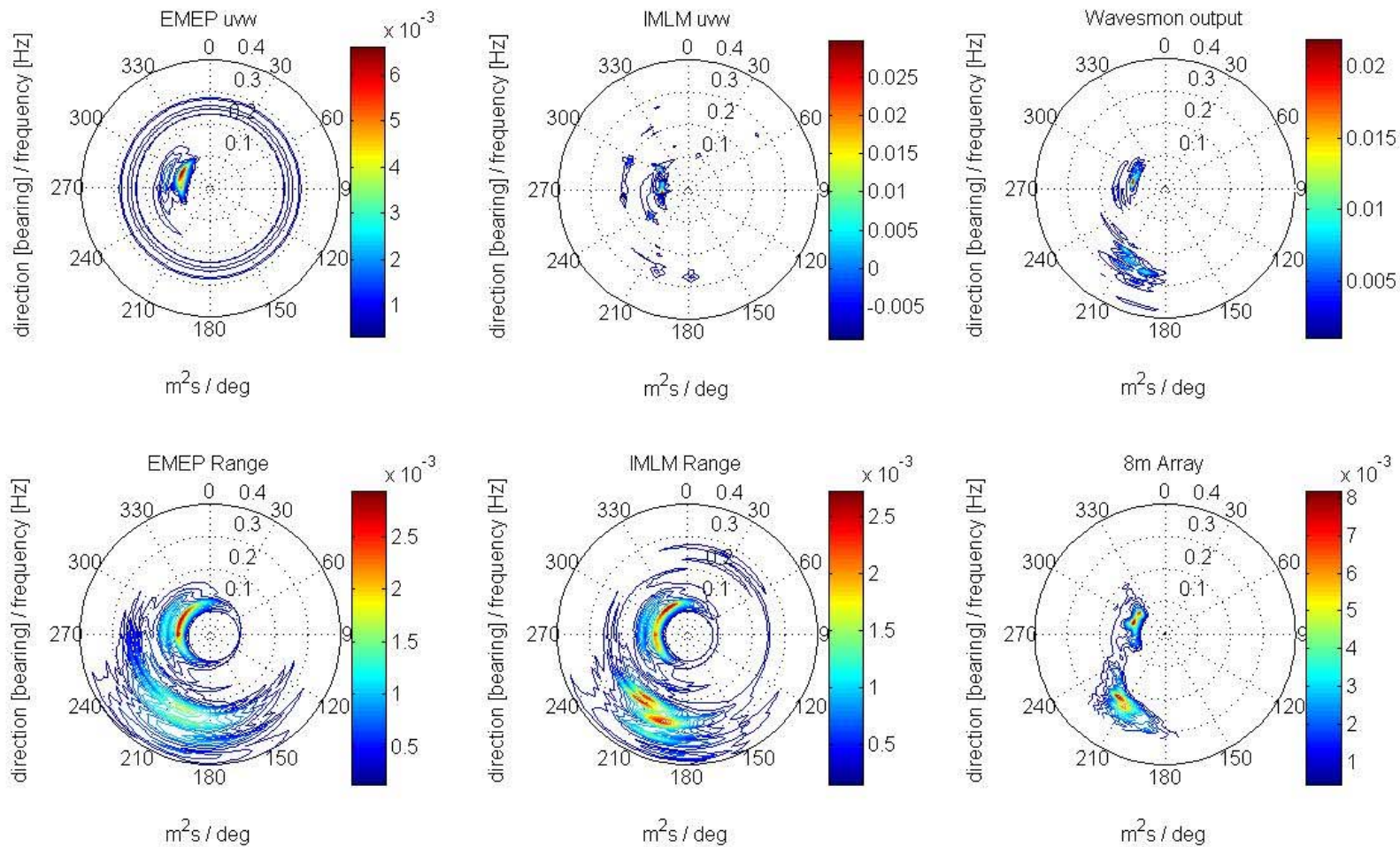


Sea surface simulation in spatial domain 3x3 km for 10 m/s case of U10, with different spreading parameter $s=10$ (a); $s=75$ (d).



$$\sigma^{(1)}(\omega) = 2^6 \pi k_0^4 \sum_{m=\pm 1} S(-2m\mathbf{k}_0) \delta(\omega - m\omega_B)$$

Wave directional distribution in relation to the radar-looking direction. The colored cardioid curves denote the directional spreading with respect to various spreading widths, which are quantified using Longuet-Higgins' parameter s . OP_1 and OP_2 represent the magnitudes of two first-order peaks associated with the receding and approaching Bragg waves to the radar site. The ratio between OP_1 and OP_2 is related to the main wave direction as well as the directional spreading width. With a narrower directional spreading (increasing s), this ratio becomes sensitive to the noise level.

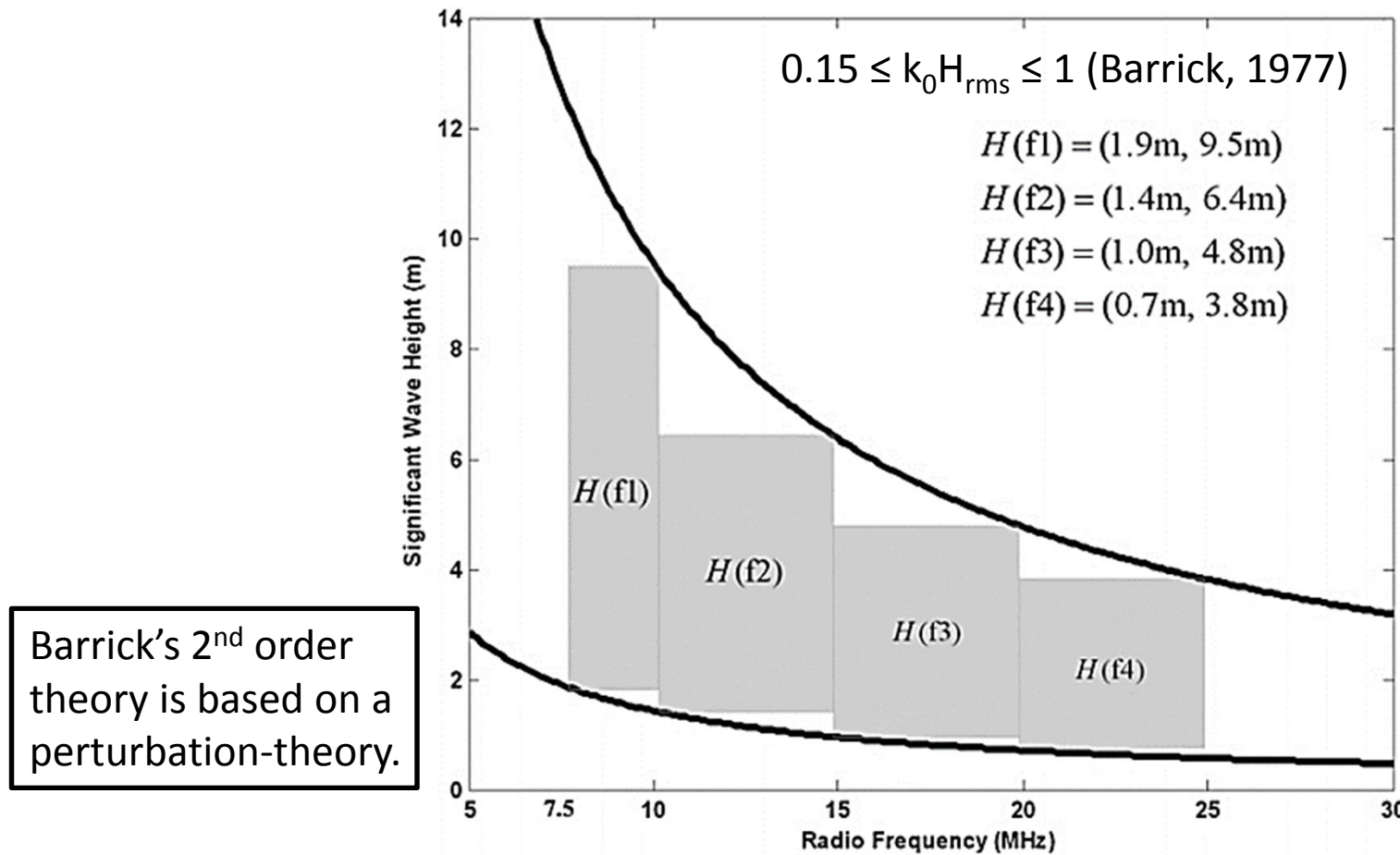


Notes: Even the measured data at sea, according to the different calculation theory and observation method, the calculation results of the direction spectrum are very different.

提醒：即便是海上實測資料，依據採用的推算理論、觀測方法的不同，方向波譜的推算結果差異很大。

- The challenge of HF observation for typhoon waves
 - Selection of Radar frequency (H_s and s)
 - Barrick's 2nd order theory is based on a perturbation-theory expansion of the nonlinear hydrodynamic and electromagnetic equations for water and waves.
 - The perturbation theory has a finite radius of convergence in the "smallness parameters". One of these is $k_o h$, where k_o is the radar spatial wavenumber and h is the rms roughness waveheight.
 - $H_{sat} = 2/k_0$, about 8 m for 12 MHz, 20 m for 5MHz
 - When choosing lower frequency band, the spreading of the corresponding Bragg wave gets narrower.

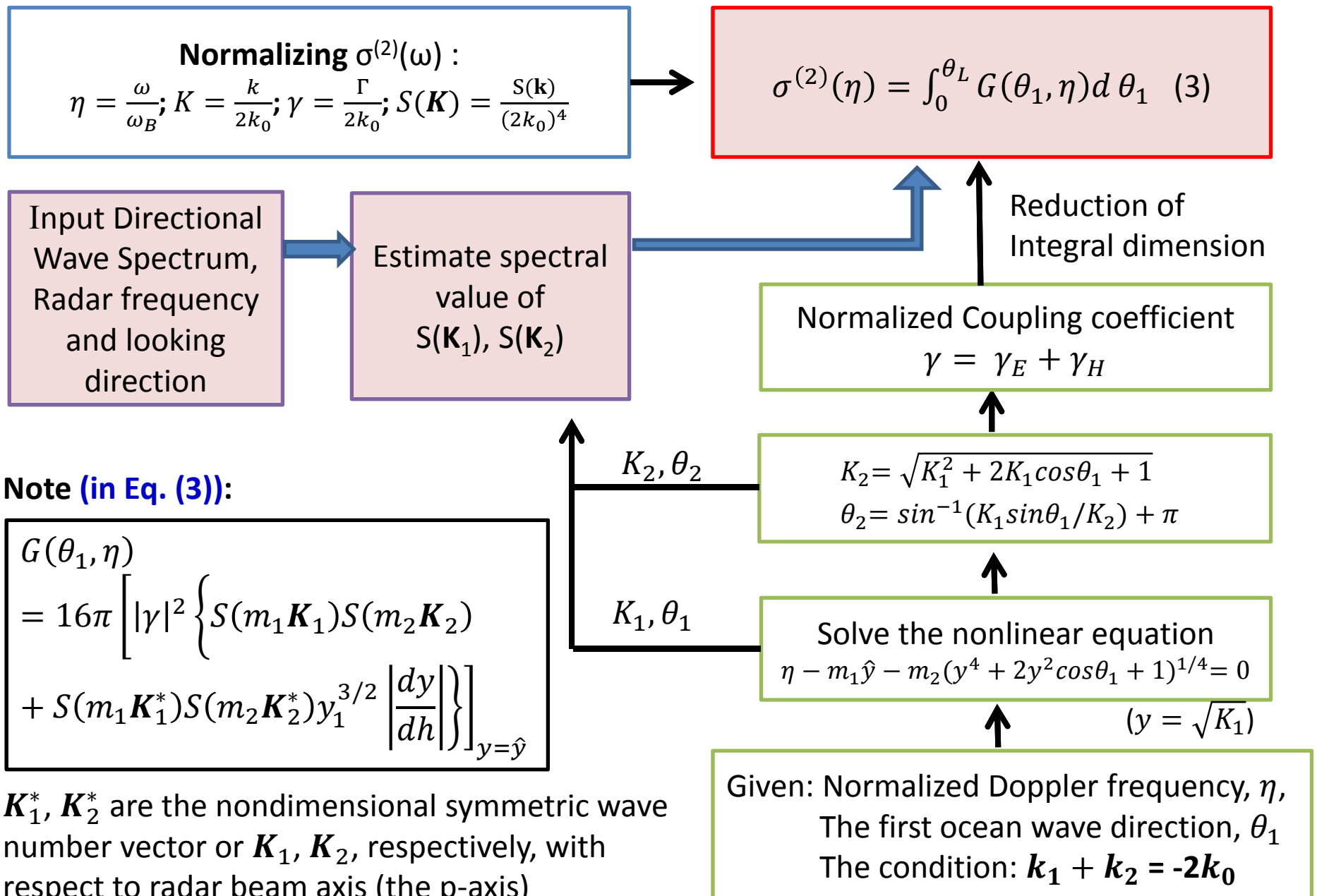
The Hs Limitation of HF radar



(Chen et. al., Journal of Atmospheric and Oceanic Technology 2013)

The perturbation theory has a finite radius of convergence in the "smallness parameters". One of these is $k_o h$, where k_o is the radar spatial wavenumber and h is the rms roughness waveheight, $H_{\text{sat}} = 2/k_o$

The 2nd order peaks simulation



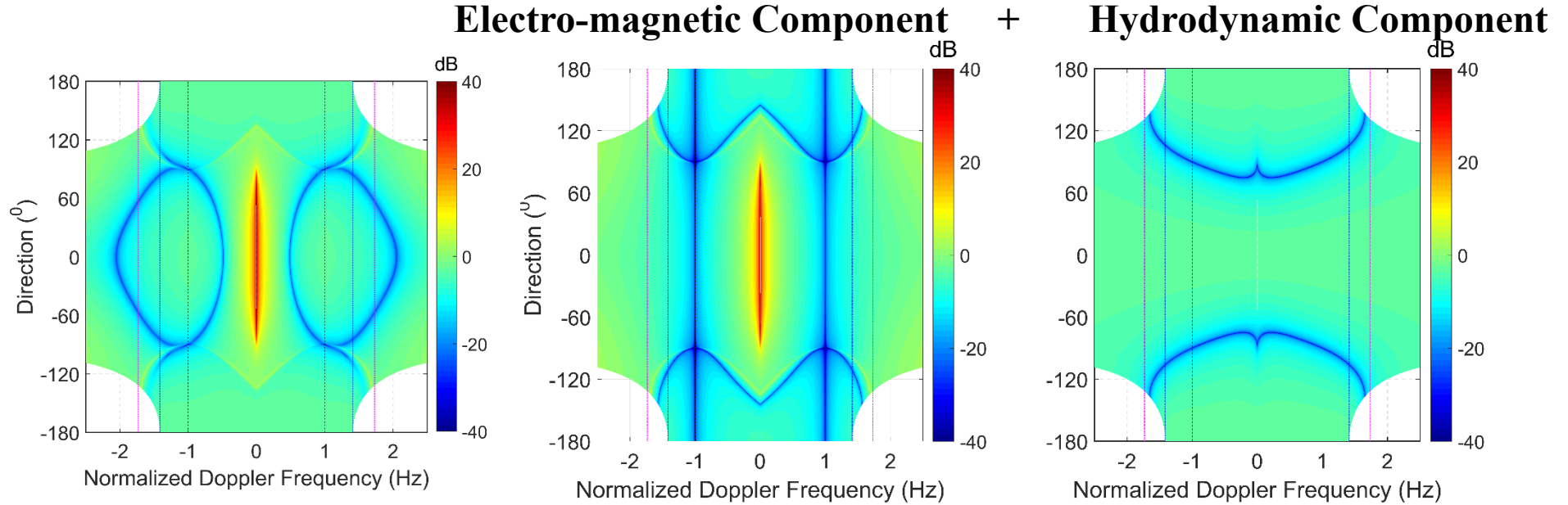
The coupling coefficient, Γ

$$\sigma^{(2)}(\omega) = 2^6 \pi k_0^4 \sum_{m_1, m_2 = \pm 1} \int_{-\infty}^{+\infty} \int_{-\infty}^{+\infty} |\Gamma|^2 S(m_1 \mathbf{k}_1) S(m_2 \mathbf{k}_2) \delta(\omega - m_1 \sqrt{gk_1} - m_2 \sqrt{gk_2}) dp dq$$

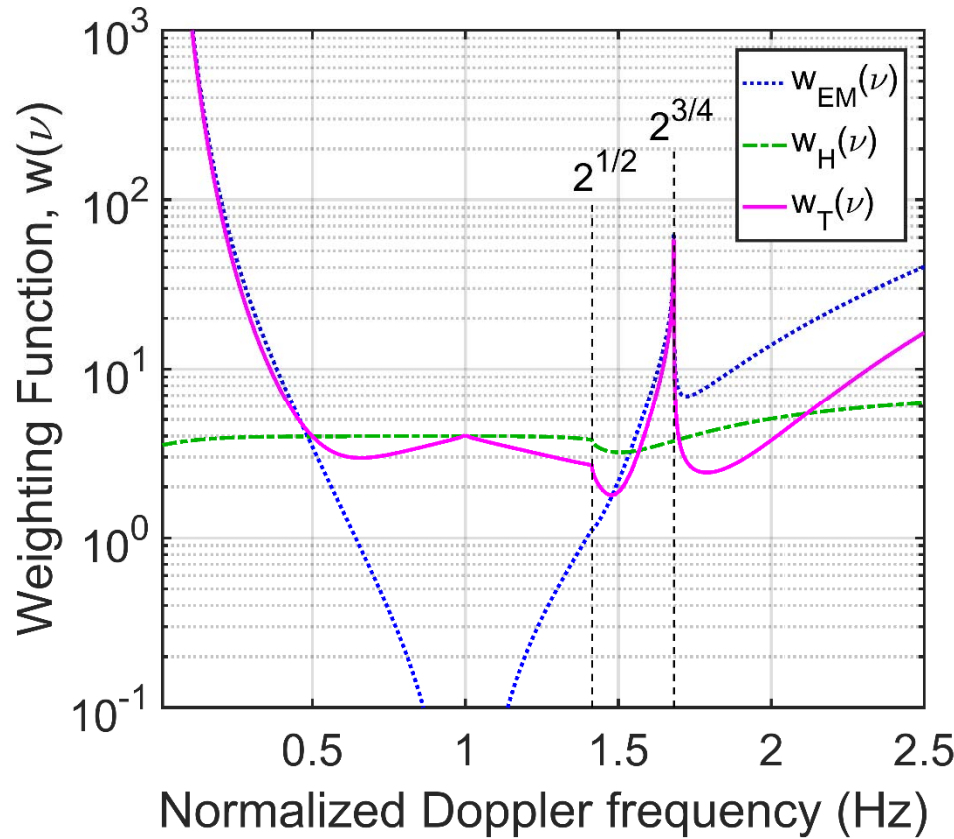
$$\Gamma_E = \frac{1}{2} \left[\frac{\frac{(\mathbf{k}_1 \cdot \mathbf{k}_0)(\mathbf{k}_2 \cdot \mathbf{k}_0)}{k_0^2} - 2\mathbf{k}_1 \cdot \mathbf{k}_2}{\sqrt{\mathbf{k}_1 \cdot \mathbf{k}_2} + k_0 \Delta} \right]$$

$$\Gamma_H = \frac{-i}{2} \left[k_1 + k_2 \frac{(k_1 k_2 - \mathbf{k}_1 \cdot \mathbf{k}_2)}{m_1 m_2 \sqrt{k_1 k_2}} \frac{(\omega^2 + \omega_B^2)}{(\omega^2 - \omega_B^2)} \right]$$

$$\Gamma = \Gamma_E + \Gamma_H$$

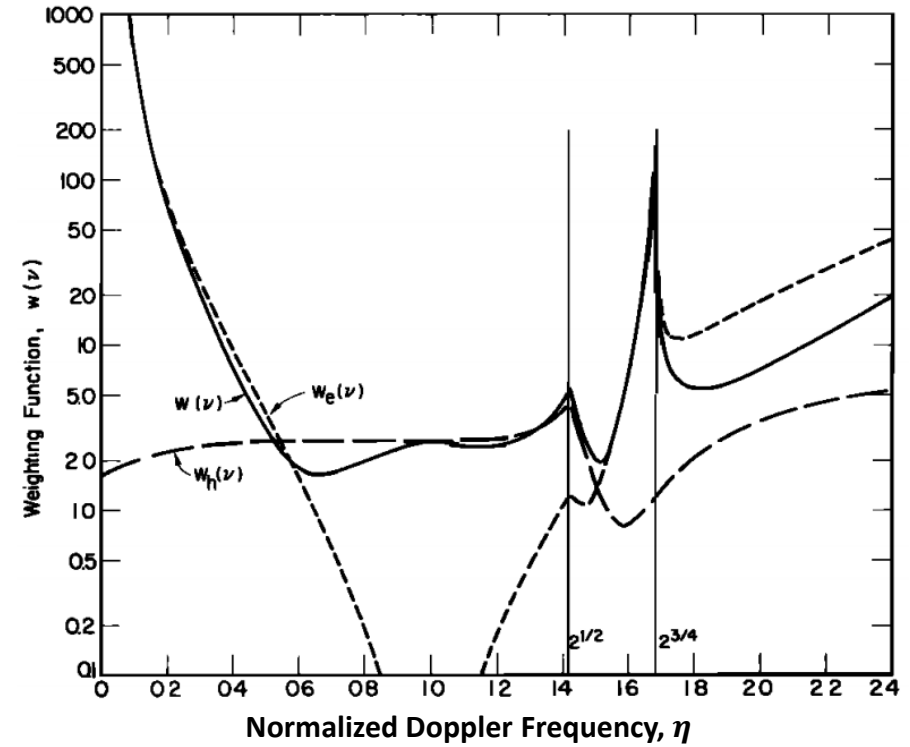


The Weighting function



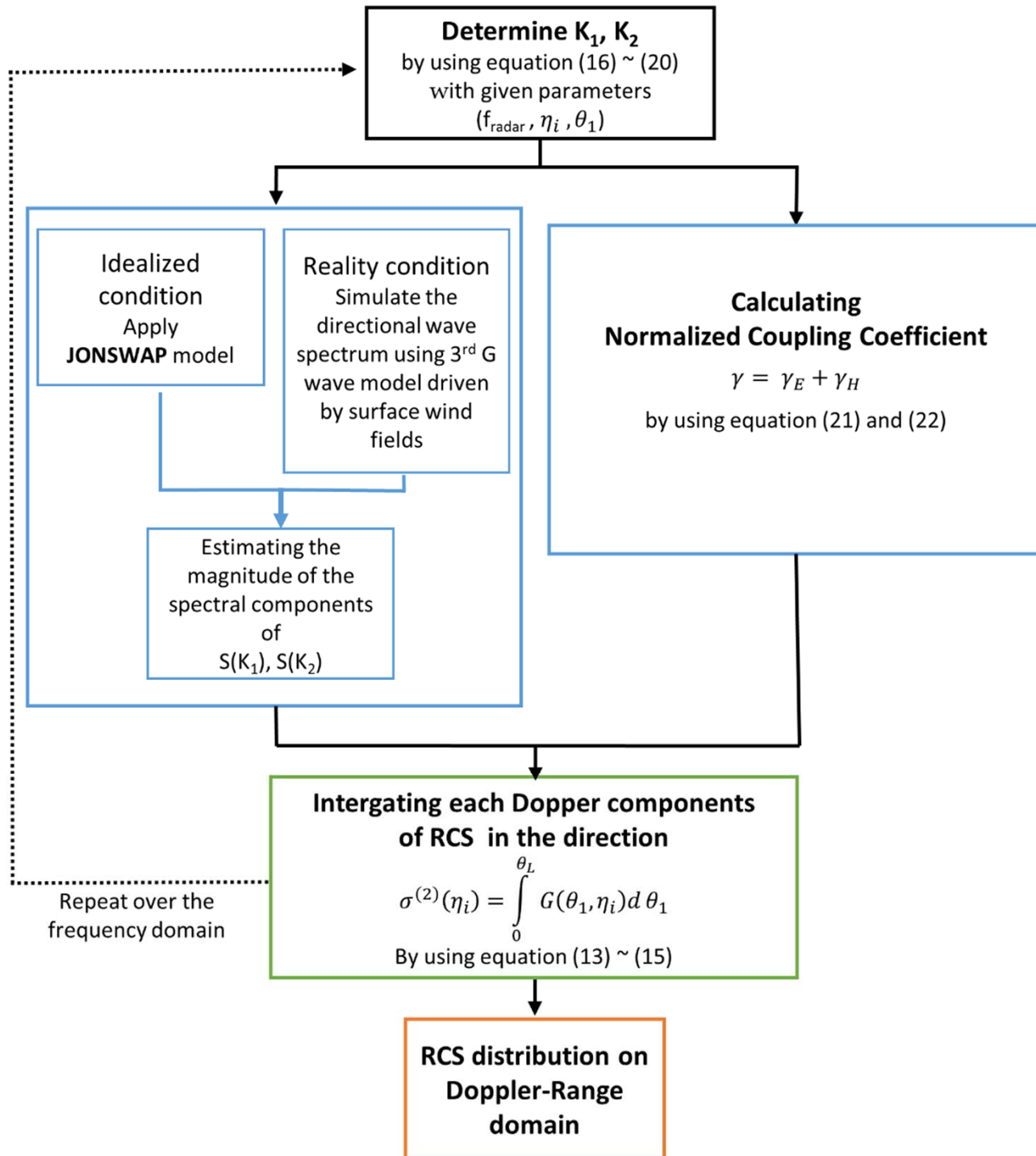
Where, $w(\eta)$ is the weighting function

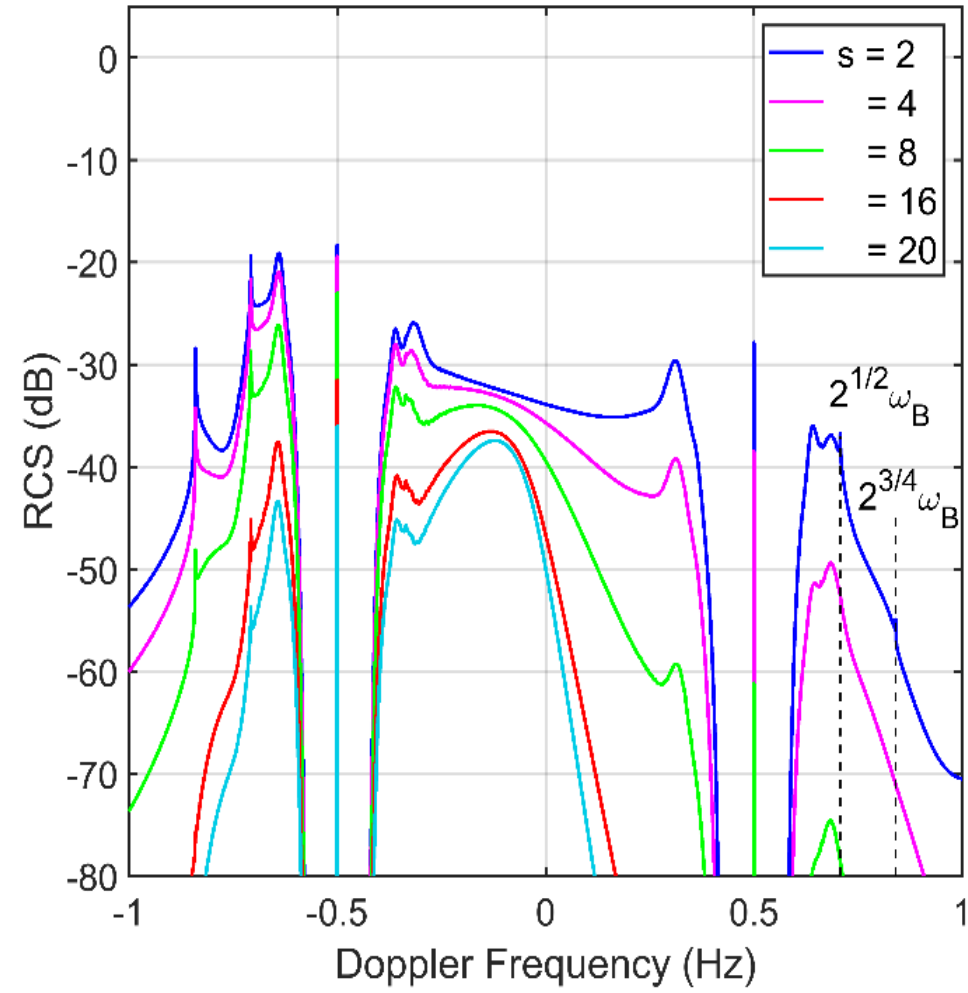
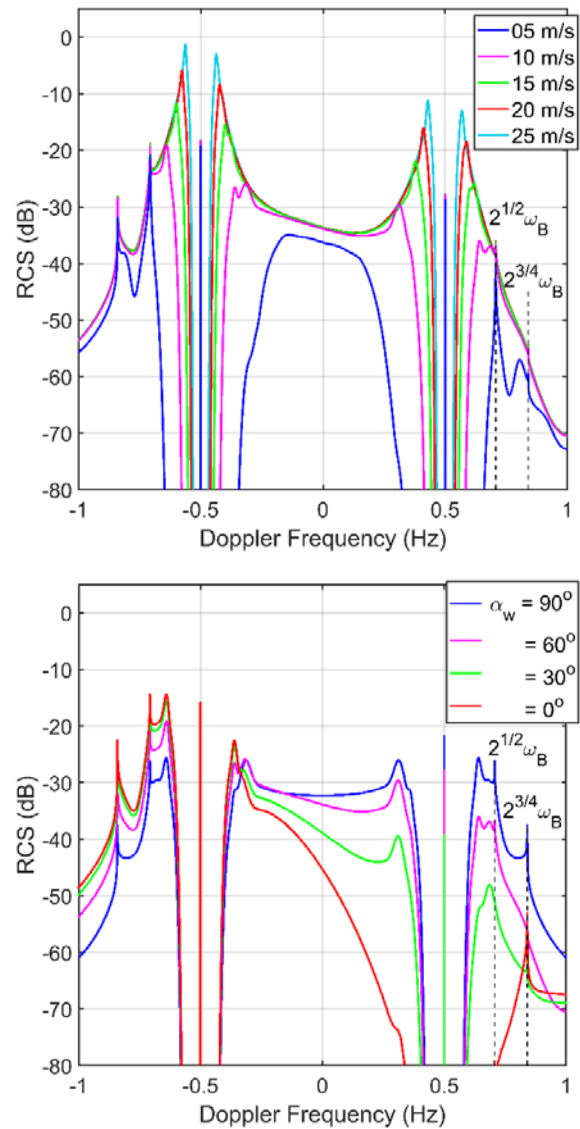
$$\left(\frac{k_0^2}{8}\right)w(\eta) = \overline{|\Gamma|^2}$$



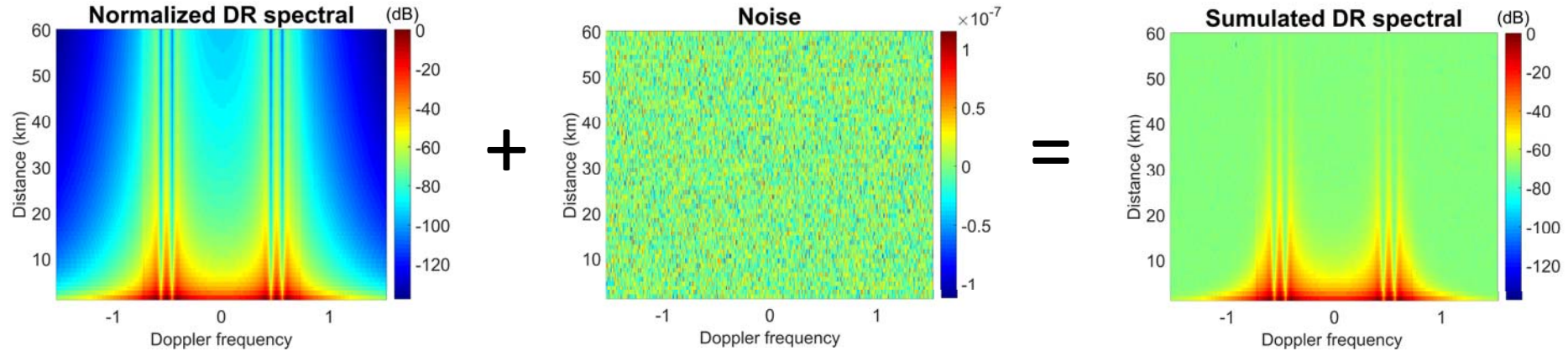
(Barrick, D.E., 1977)

The Simulation Toolbox

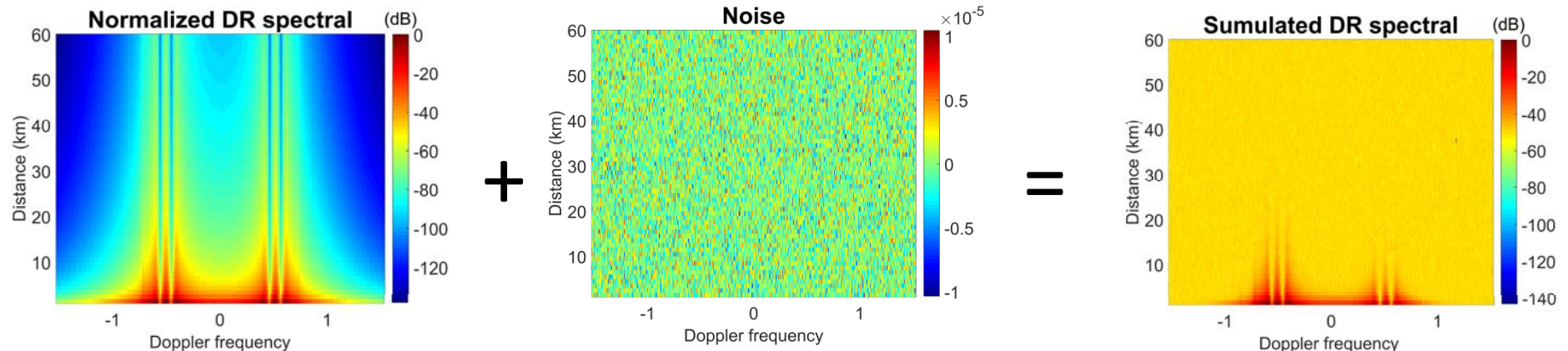




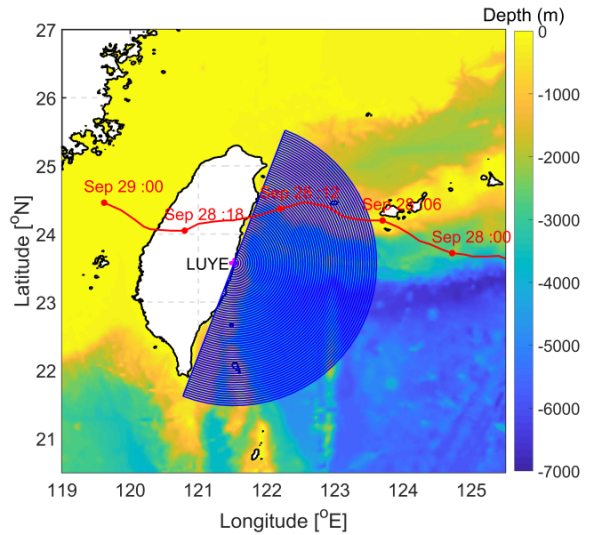
Simulation of D-R spectra As Given Targets for Method Performance Assessment



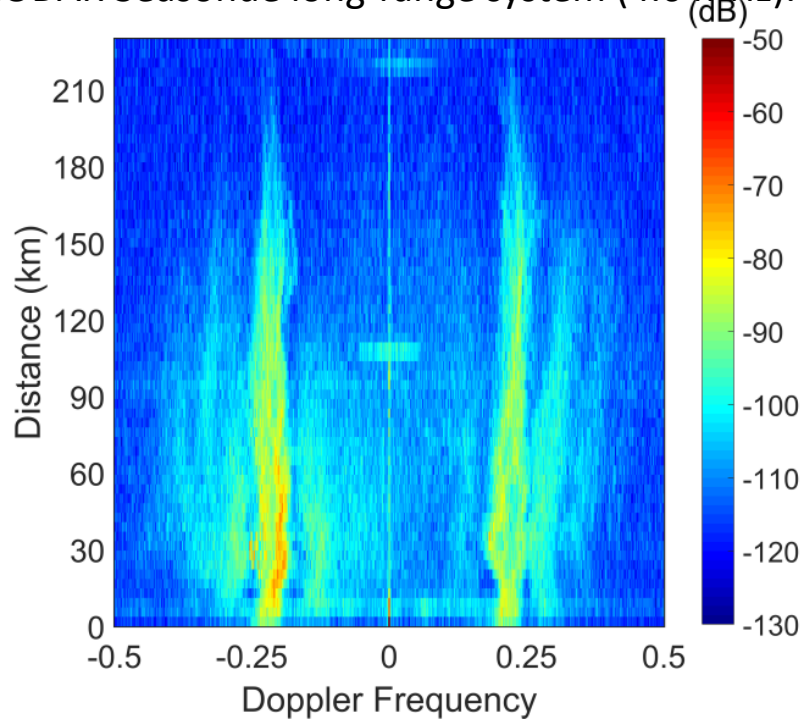
(Wave-to-Radar-Look = 85^0 , Spreading $s = 2$, $f_{radar} = 25\text{MHz}$, Noise -70dB)



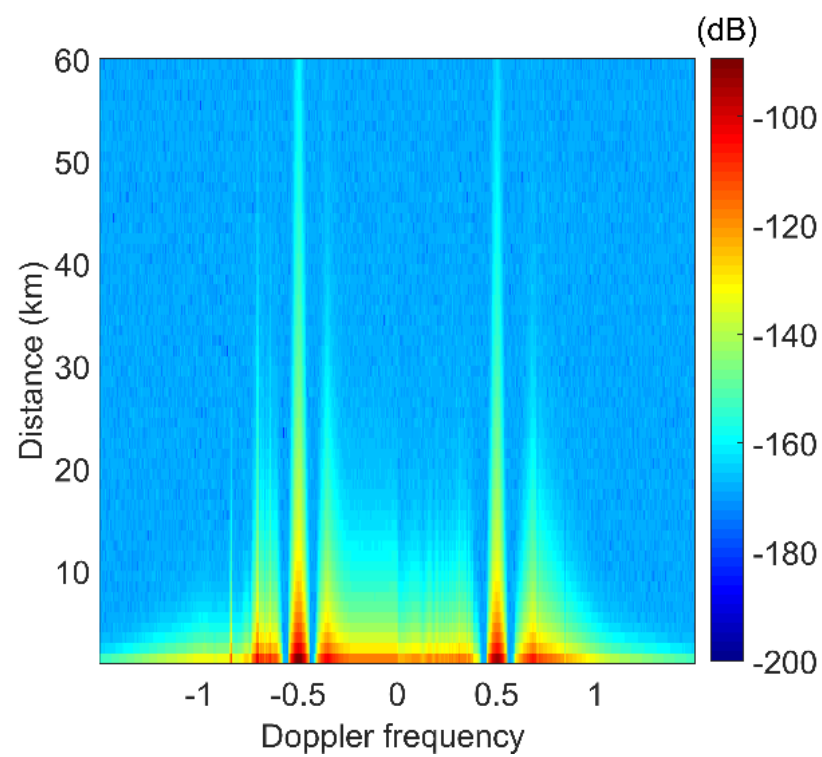
(Wave-to-Radar-Look = 60^0 , Spreading $s = 2$, $f_{radar} = 25\text{MHz}$, Noise -50dB)



Obtained at LuYe station at 0600LT Sep 28 2015. The LUYE station is equipped with CODAR Seasonde long-range system (4.6 MHz).



An example of simulated DR spectrum at the time when Typhoon Dujuan made landfall. The simulated Doppler-Range spectra was generated using JONSWAP spectral form and Longuet-Higgins' directional spreading function with $\alpha_w = 60^\circ$, $\theta_N = 60^\circ$, and $U_{10} = 25$ m/s. Operating frequency of radar system is 4.6 MHz, range resolution is 3.7 km, and SNR = -70 dB.



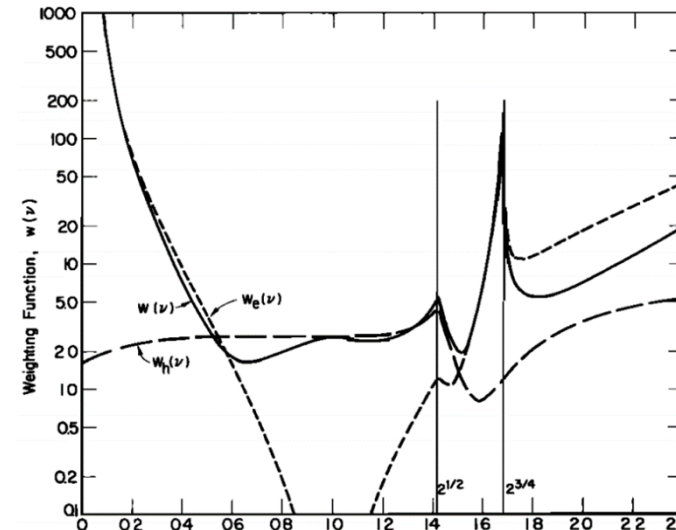
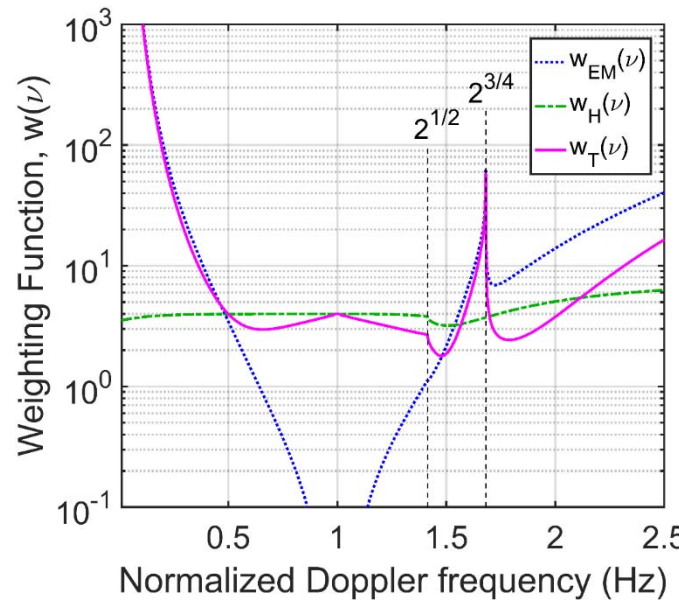
Methods for Retrieval of Hs and Tm (monostatic case)

$$k_0 h_{rms} = \left[2 \frac{\int_{-\infty}^{\infty} \sigma^{(2)}(\omega) w^{-1}(\eta) d\omega}{\int_{-\infty}^{\infty} \sigma^{(1)}(\omega) d\omega} \right]^{1/2} \quad (4)$$

$$\frac{\omega_B T_m}{2\pi} = \frac{\int_{0,1}^{1,\infty} \sigma^{(2)}(\omega) w^{-1}(\eta) d\eta}{\int_{0,1}^{1,\infty} |\eta - 1| \sigma^{(2)}(\omega) w^{-1}(\eta) d\eta} \quad (5)$$

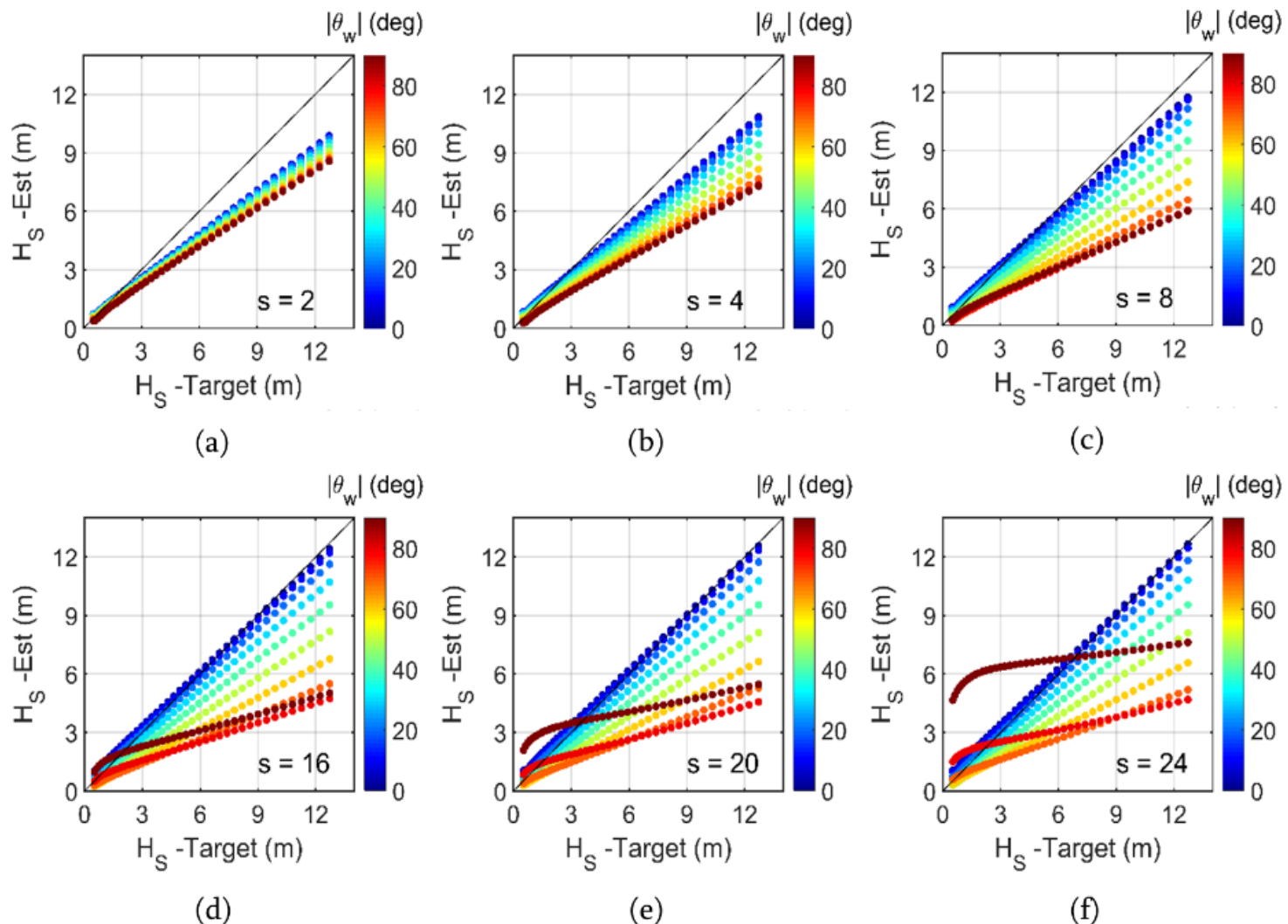
[\(Barrick, D.E., 1977\)](#)

Where, $w(\eta)$ is the weighting function $\left(\frac{k_0^2}{8}\right) w(\eta) = \overline{|\Gamma|^2}$



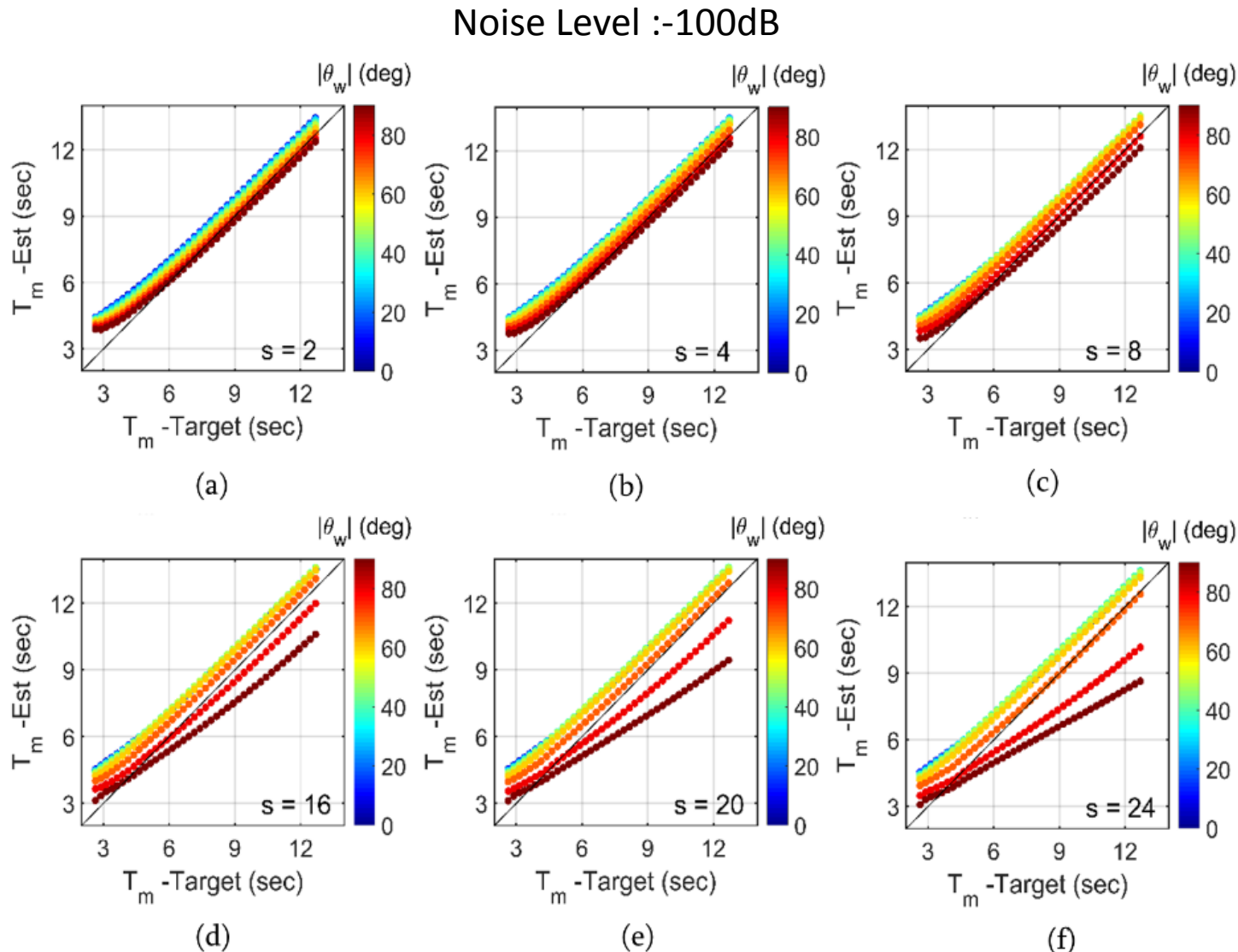
Sensitivity of Wave Height Estimation

Noise Level :-100dB



The errors of H_s estimation using Barrick's formula depend on θ_w and the directional spreading parameter s

Sensitivity of Period Estimation



The errors of T_m estimation using Barrick's formula depend on θ_w and the directional spreading parameter s at wave Bragg frequency

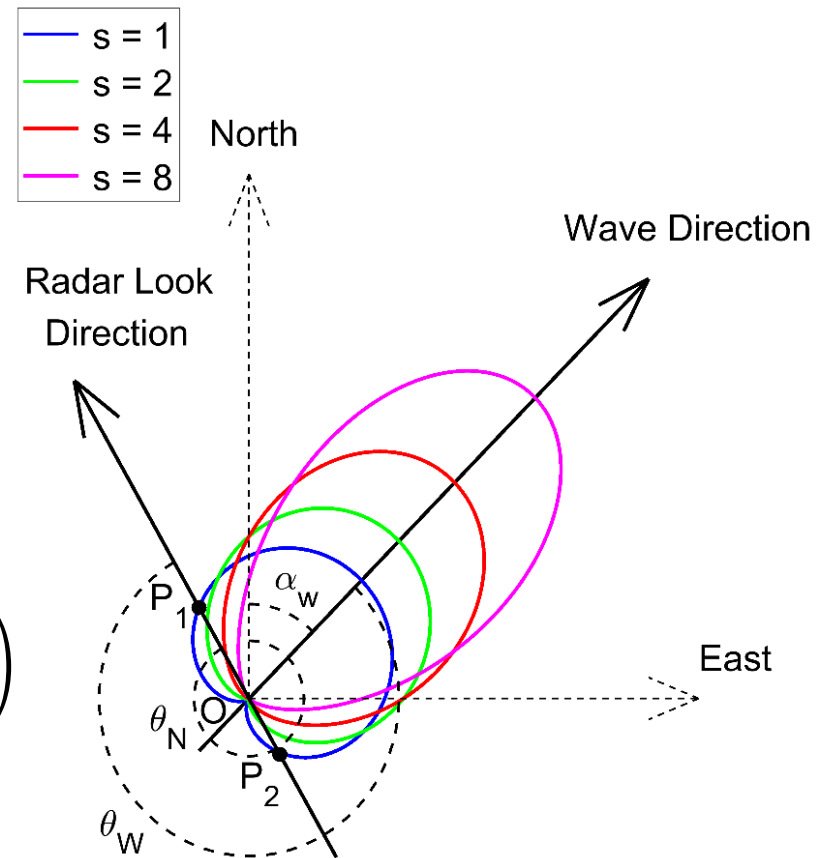
The retrieval of wave directionality

- Replace Directional Spreading Function into $(\sigma^{(1)})$

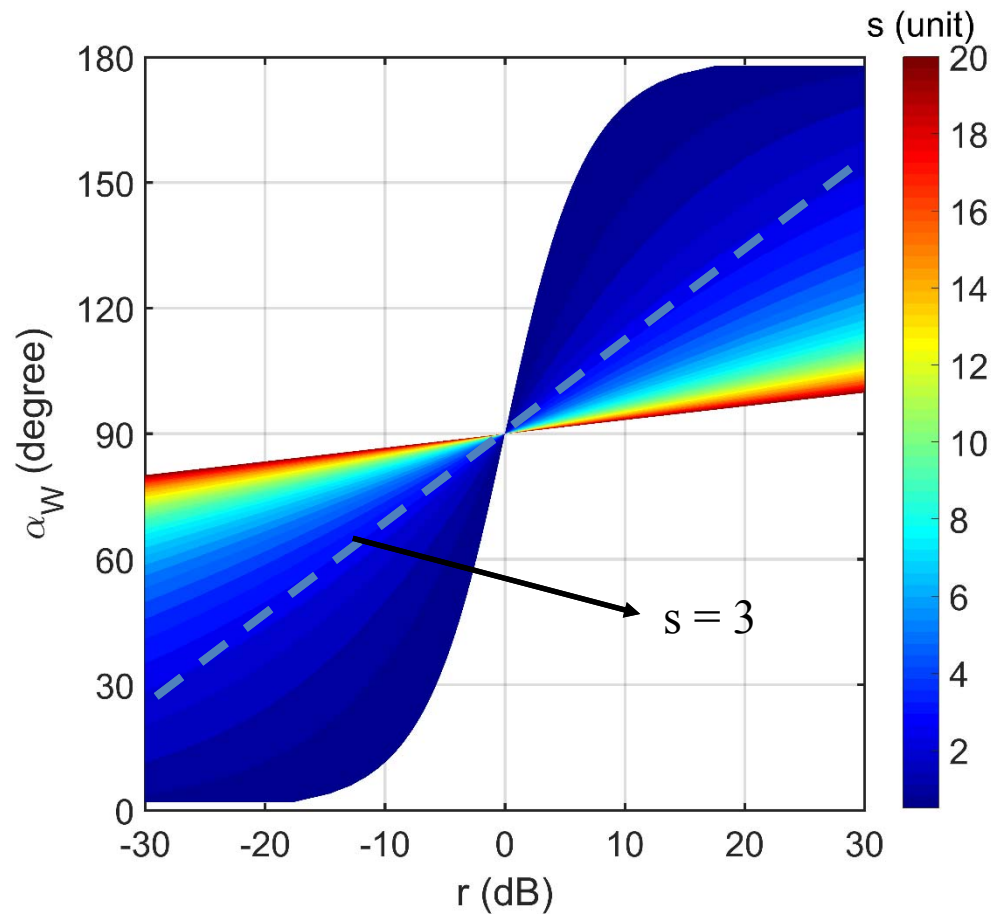
$$\left\{ \begin{array}{l} \sigma^{(1)}(-\omega_B) = 2^6 \pi k_0^4 F(2k_0) G\left(\frac{\theta_N - \alpha_w}{2}\right) \\ \sigma^{(1)}(+\omega_B) \\ = 2^6 \pi k_0^4 F(-2k_0) G\left(\frac{\pi + \theta_N - \alpha_w}{2}\right) \end{array} \right.$$

$$\begin{aligned} r &= 10 \log_{10} \left(\frac{B^+}{B^-} \right) \\ &= 10 \log_{10} \left(\frac{\sigma_1(\omega_B)}{\sigma_1(-\omega_B)} \right) = 10 \log_{10} \left(\frac{G(\pi + \theta_N - \alpha_w)}{G(0 + \theta_N - \alpha_w)} \right) \end{aligned}$$

$$r = 10 \log_{10} \left(\tan^{2s} \frac{|\theta_w|}{2} \right) \quad (6)$$



Cardioid Signal θ_w shows the noise effect can be influential for cases of narrower angular spreading (and also the radio wave frequency)

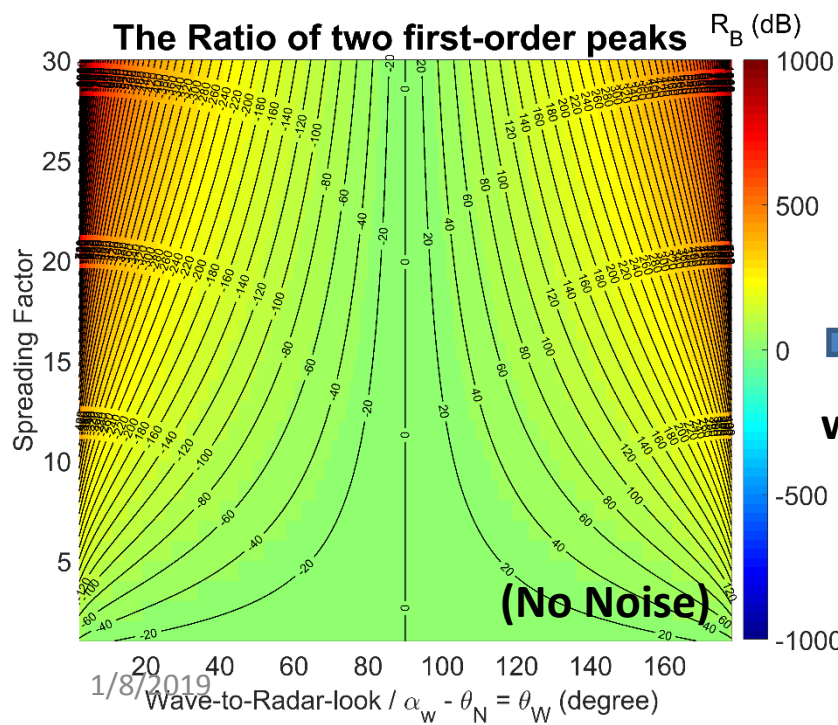


The relationship between the angle of wave-to-radar looking and the ratio of two first-order peaks under different spreading parameters for radar-looking direction $\theta_N = 0^\circ$ and $\alpha_w = 0^\circ - 180^\circ$

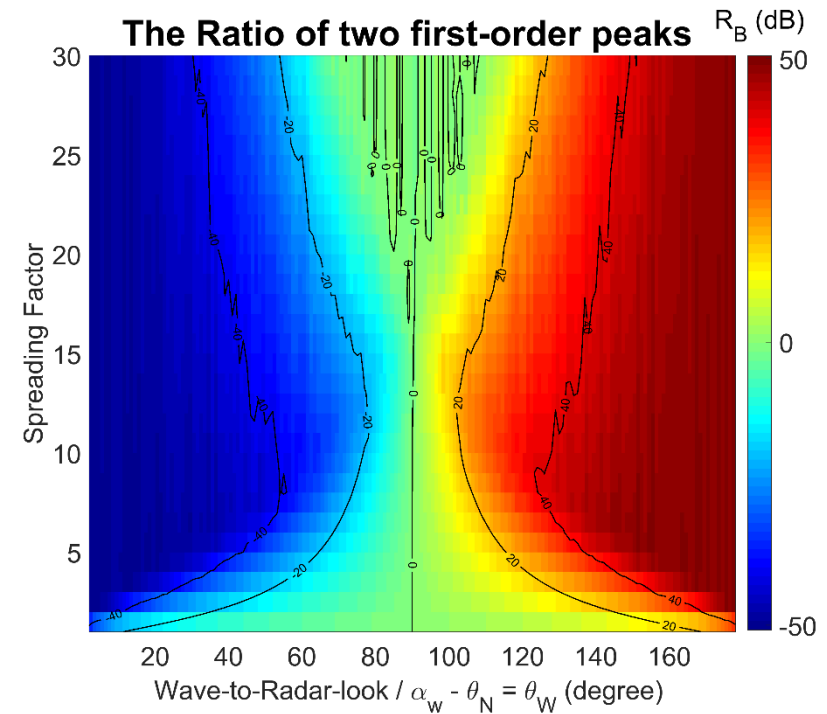
How the noise could effect the S and θ_w ?

Replace by the direction spreading model Longuet-Higgins et. al, (1963)

$$\rightarrow r = 10 \log_{10} \left(\tan^2 s \frac{|\theta_w|}{2} \right)$$



with noise



Solving directionality using nonlinear interation method

(Dual-radar case)

For Radar-1 $r_1 = 10 \log_{10} \left(\tan^2 s \frac{|\alpha_w - \theta_{N1}|}{2} \right)$

$$\rightarrow \alpha_w = \theta_{N1} \pm 2 \tan^{-1} \left(10^{\frac{r_1}{20s}} \right)$$

For Radar-2 $r_2 = 10 \log_{10} \left(\tan^2 s \frac{|\alpha_w - \theta_{N2}|}{2} \right)$

$$\rightarrow \alpha_w = \theta_{N2} \pm 2 \tan^{-1} \left(10^{\frac{r_2}{20s}} \right)$$

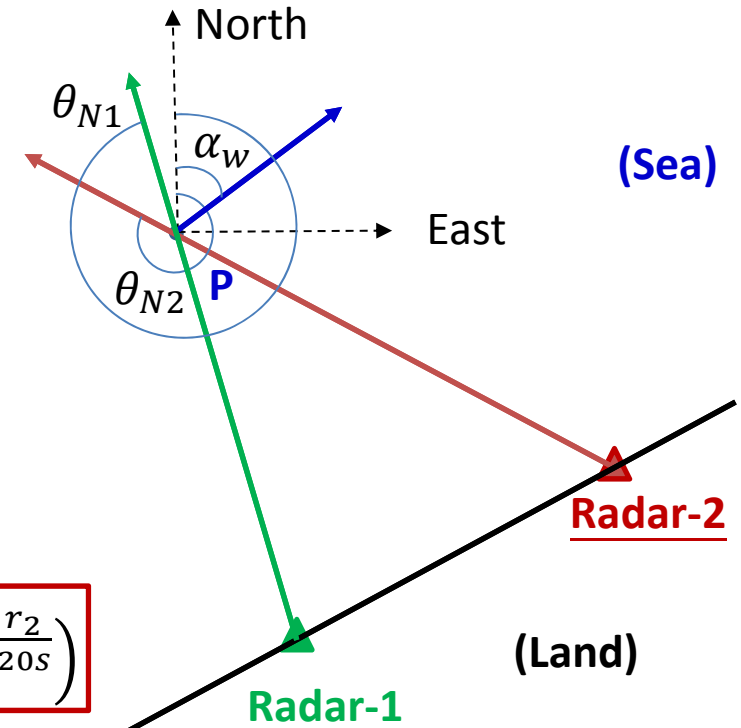
$\rightarrow \boxed{\theta_{N1} \pm 2 \tan^{-1} \left(10^{\frac{r_1}{20s}} \right) = \theta_{N2} \pm 2 \tan^{-1} \left(10^{\frac{r_2}{20s}} \right)}$

$$\theta_{N1} - \theta_{N2} + 2 \tan^{-1} \left(10^{\frac{r_1}{20s}} \right) - 2 \tan^{-1} \left(10^{\frac{r_2}{20s}} \right) = 0$$

$$\theta_{N1} - \theta_{N2} - 2 \tan^{-1} \left(10^{\frac{r_1}{20s}} \right) - 2 \tan^{-1} \left(10^{\frac{r_2}{20s}} \right) = 0$$

$$\theta_{N1} - \theta_{N2} + 2 \tan^{-1} \left(10^{\frac{r_1}{20s}} \right) + 2 \tan^{-1} \left(10^{\frac{r_2}{20s}} \right) = 0$$

$$\theta_{N1} - \theta_{N2} - 2 \tan^{-1} \left(10^{\frac{r_1}{20s}} \right) - 2 \tan^{-1} \left(10^{\frac{r_2}{20s}} \right) = 0$$



- Solve 's' first.
- With the increasing Noise Level, the S diverge.

Solving Eq. (10) using nonlinear interation method (next)

(Dual-radar case)

1. Using `fsolve.m` to obtain 4 values of 's' from each equation.
2. Remove unrealistic solutions.

3. Check Angle Ambiguity

4. Obtain the Solution of Spreading Factor of Bragg Wave

$$\alpha_{w1k} = \theta_{N1} + 2\tan^{-1}\left(10^{\frac{r_1}{20s_{est(k)}}}\right)$$

$$\alpha_{w2k} = \theta_{N1} - 2\tan^{-1}\left(10^{\frac{r_1}{20s_{est(k)}}}\right)$$

$$\alpha_{w3k} = \theta_{N2} + 2\tan^{-1}\left(10^{\frac{r_2}{20s_{est(k)}}}\right)$$

$$\alpha_{w4k} = \theta_{N2} - 2\tan^{-1}\left(10^{\frac{r_2}{20s_{est(k)}}}\right)$$

$$d\alpha_{ij} = |\alpha_{wi} - \alpha_{wj}|$$

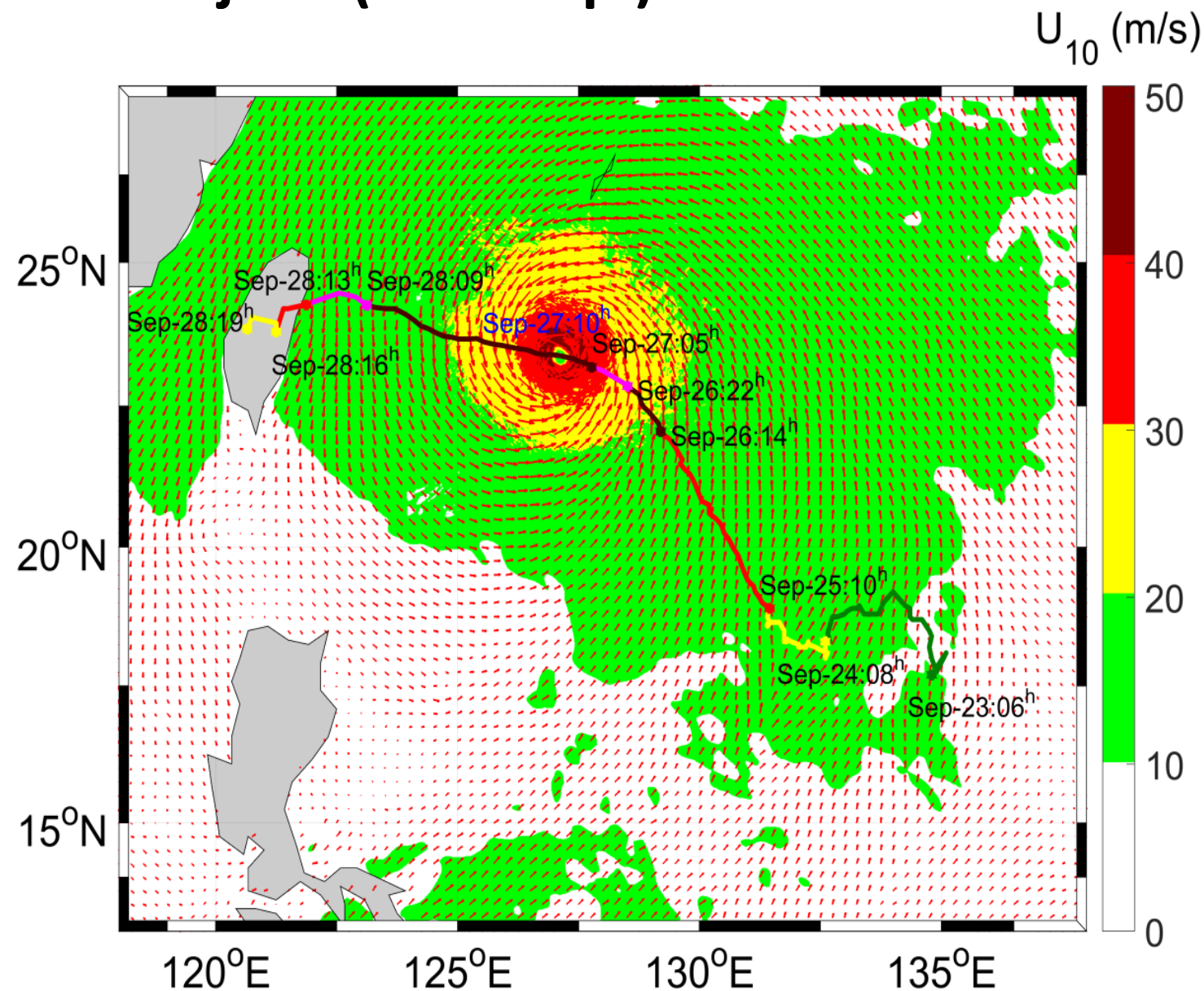
$i = [1:16]; j = [1:16]$

Determine the optimal value of $d\alpha_{ij}$

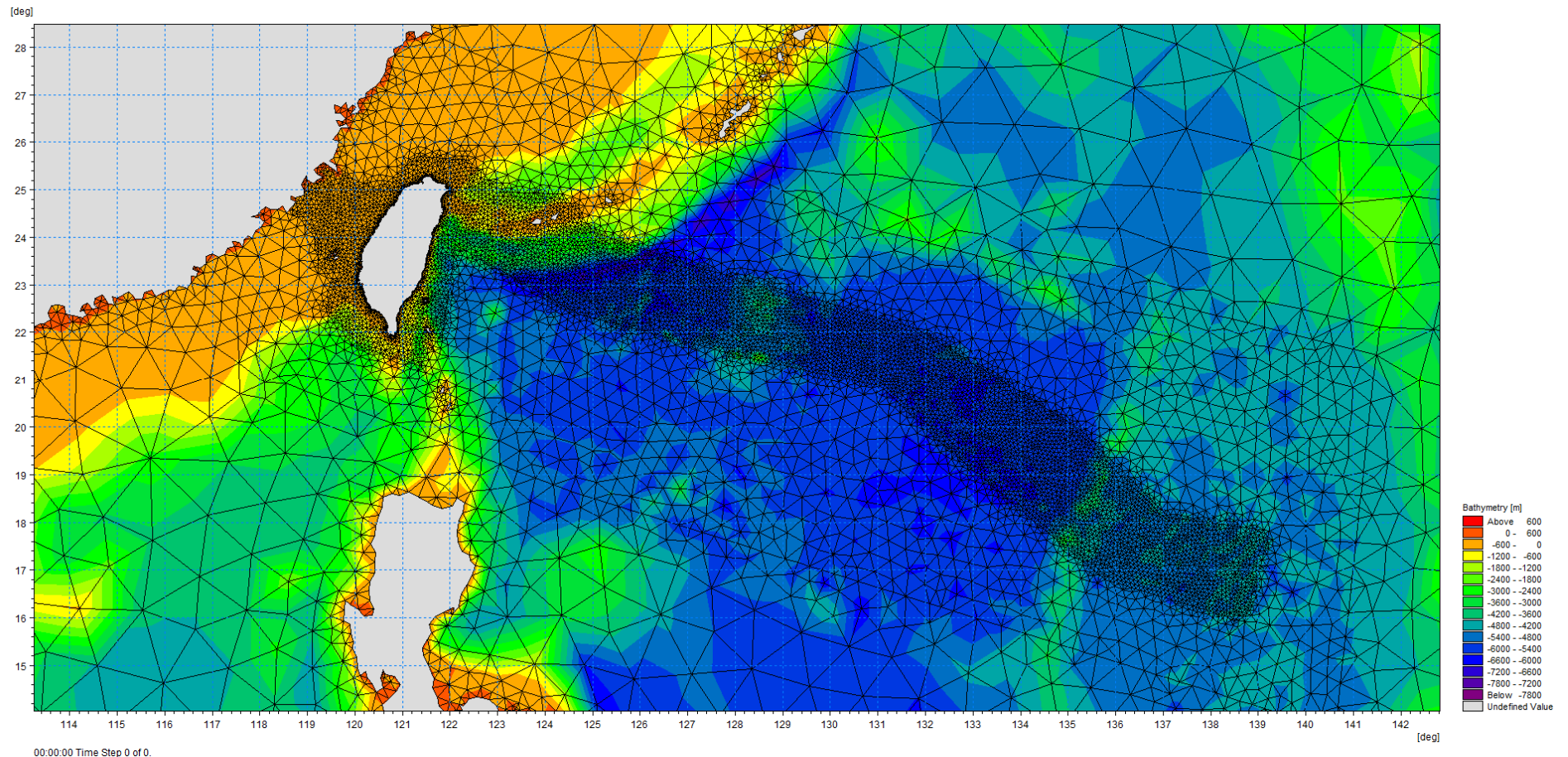
Obtaine the direction of Bragg wave

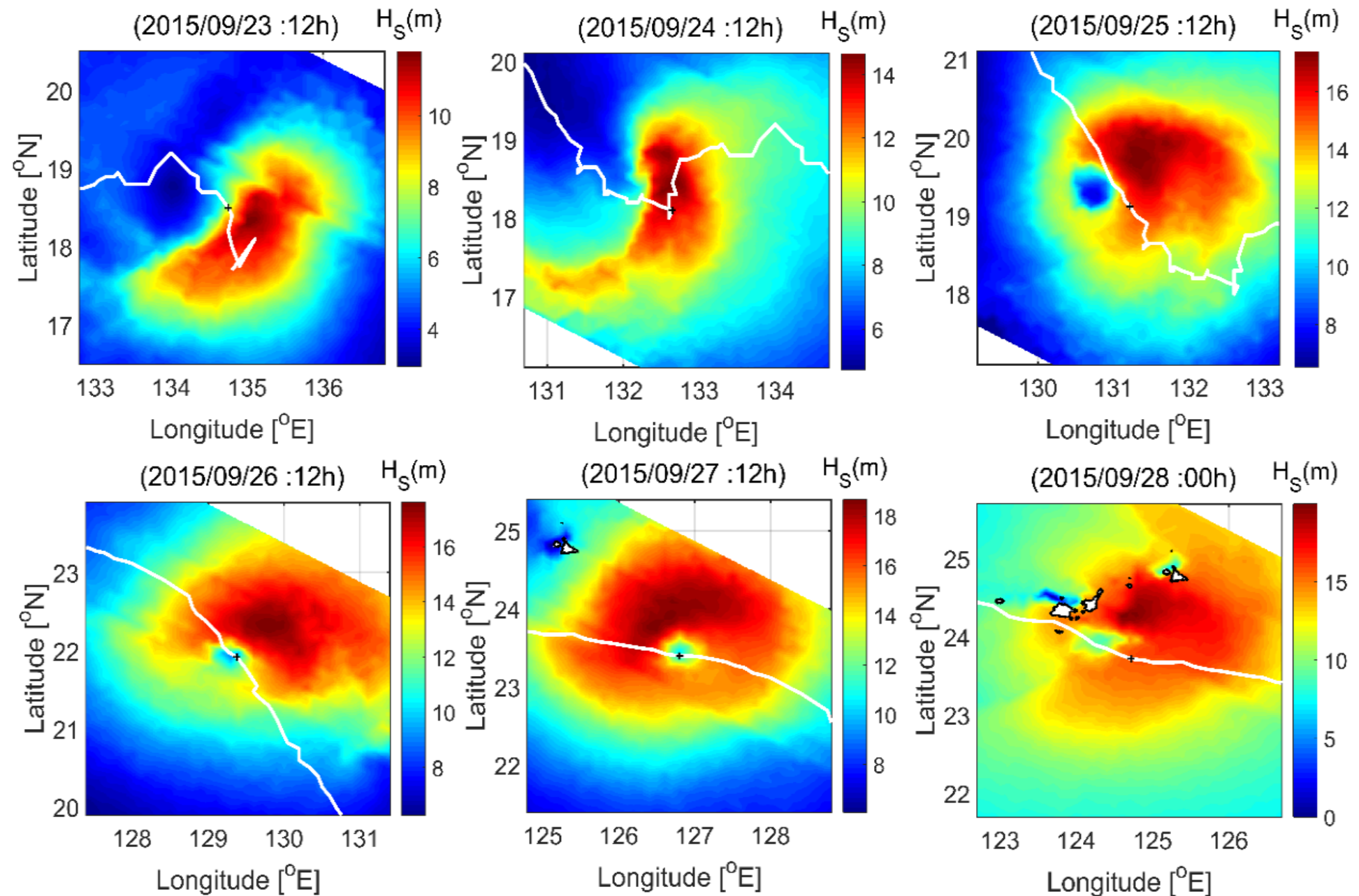
$$\alpha_w = \frac{1}{2}(\alpha_{wi} + \alpha_{wj})$$

Typhoon Dujuan (2015 Sep.)

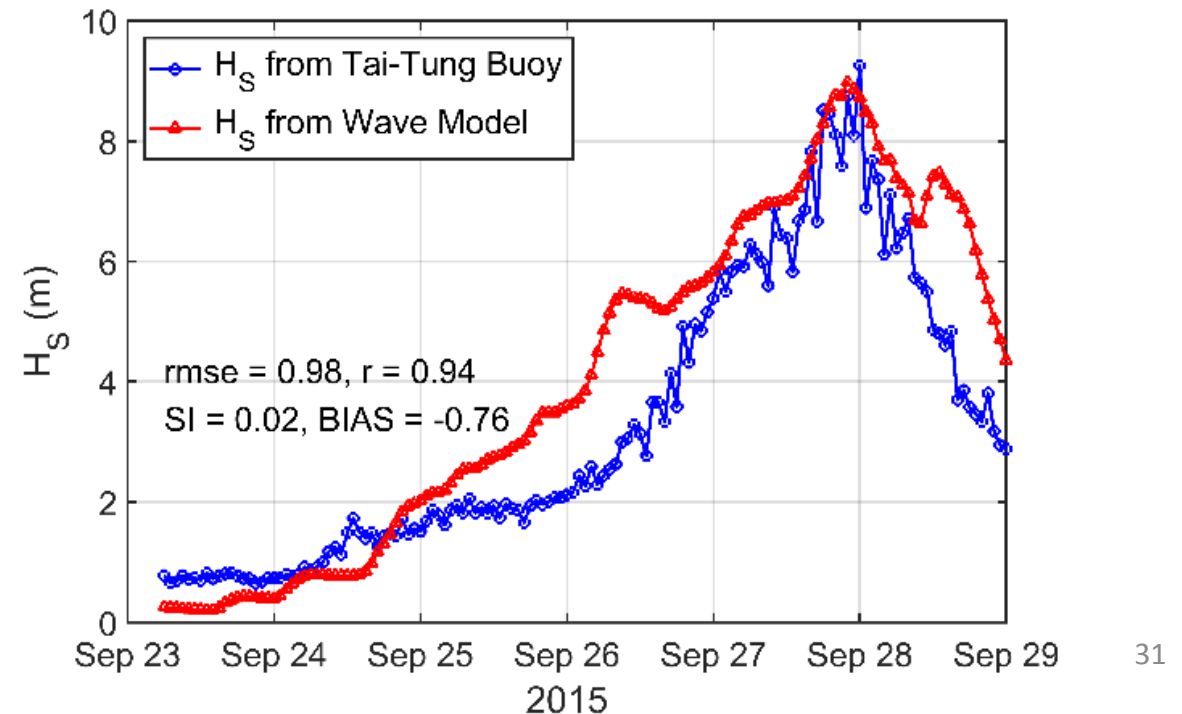
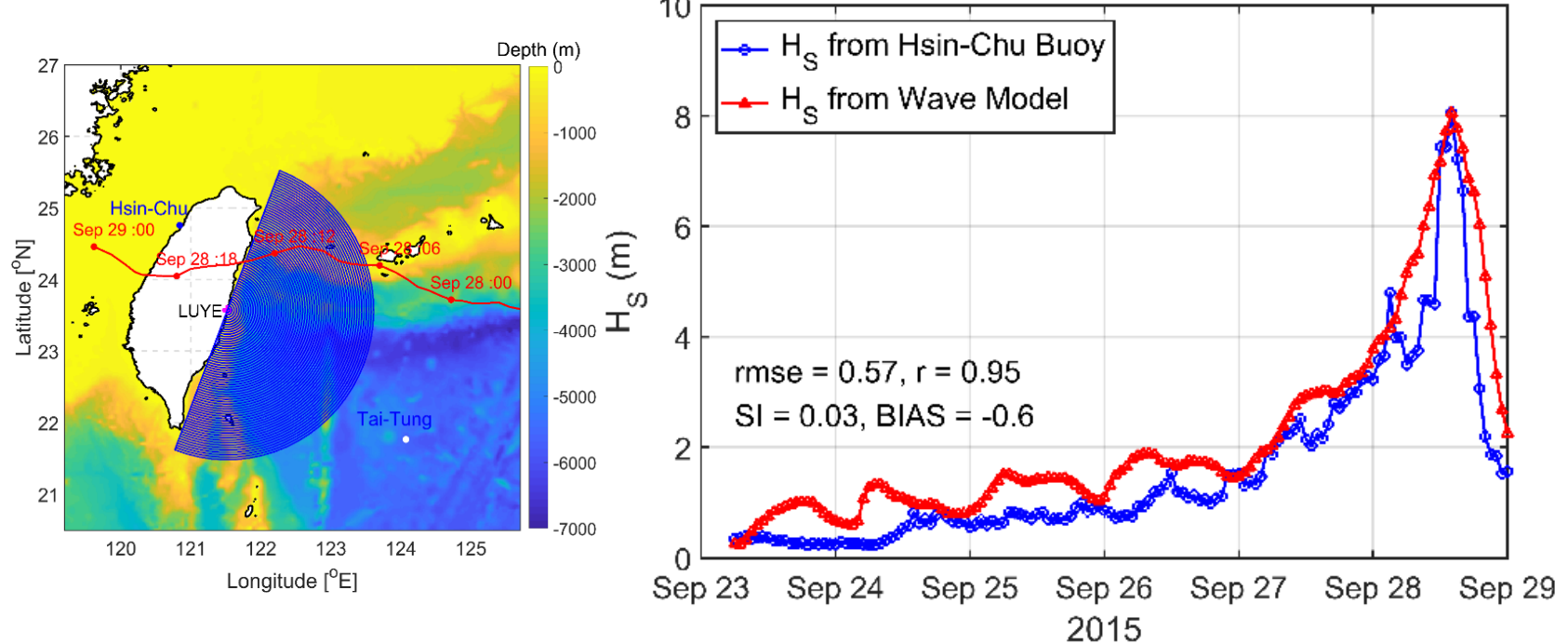


Directional Spectrum Hindcast using 3rd G Wave model on un-structure grid

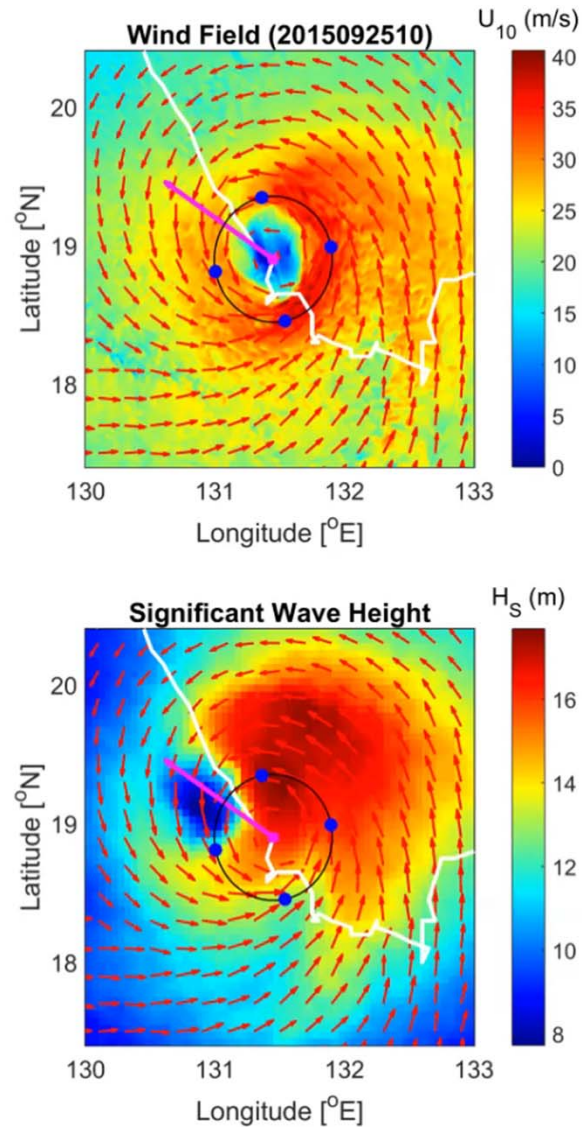




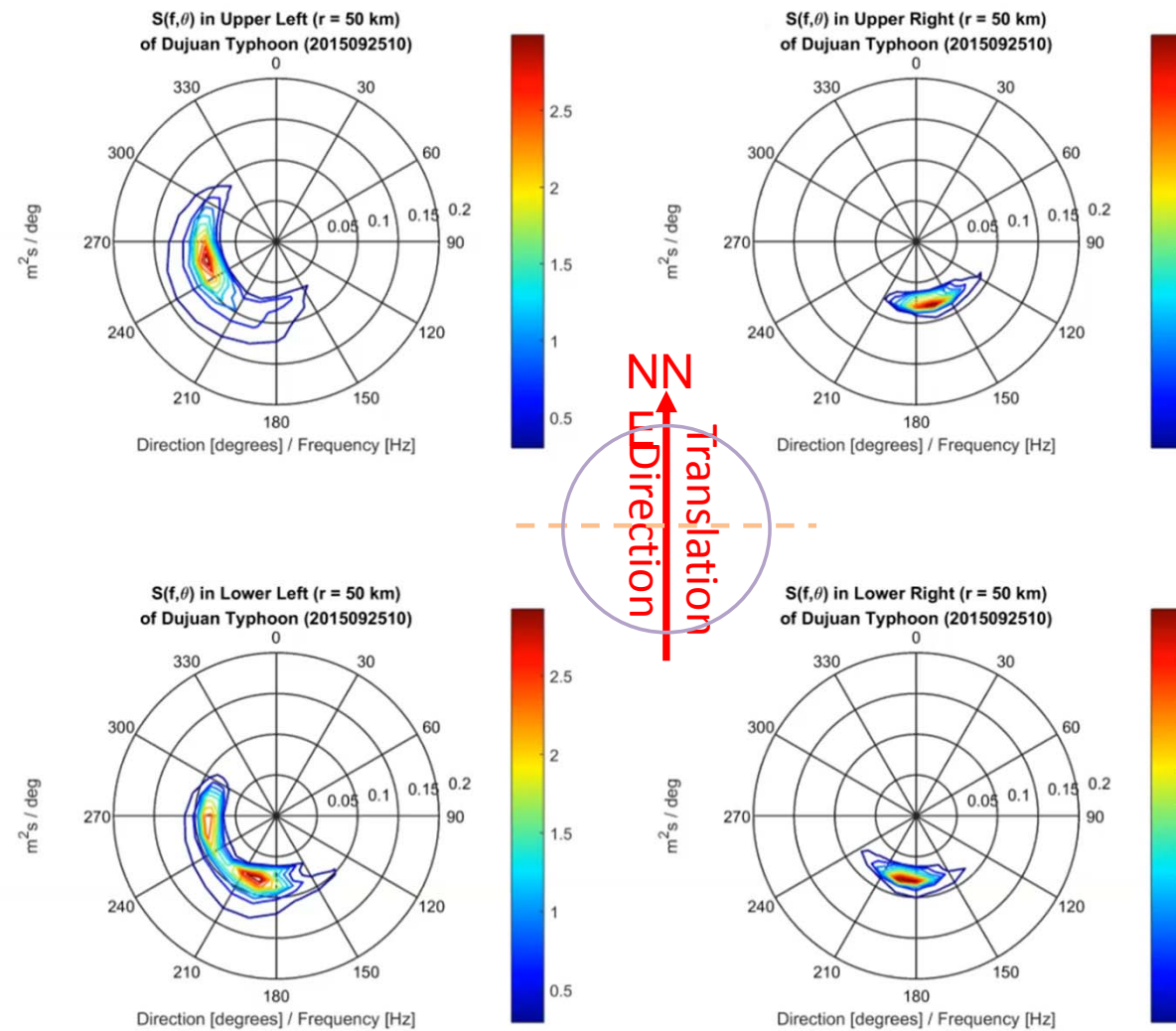
Spatial distributions of the hindcasted significant wave height around the typhoon center from September 23–28, 2015. The white line represents the trajectory of Typhoon Dujuan; the black cross denotes the position of the typhoon eye in each panel.



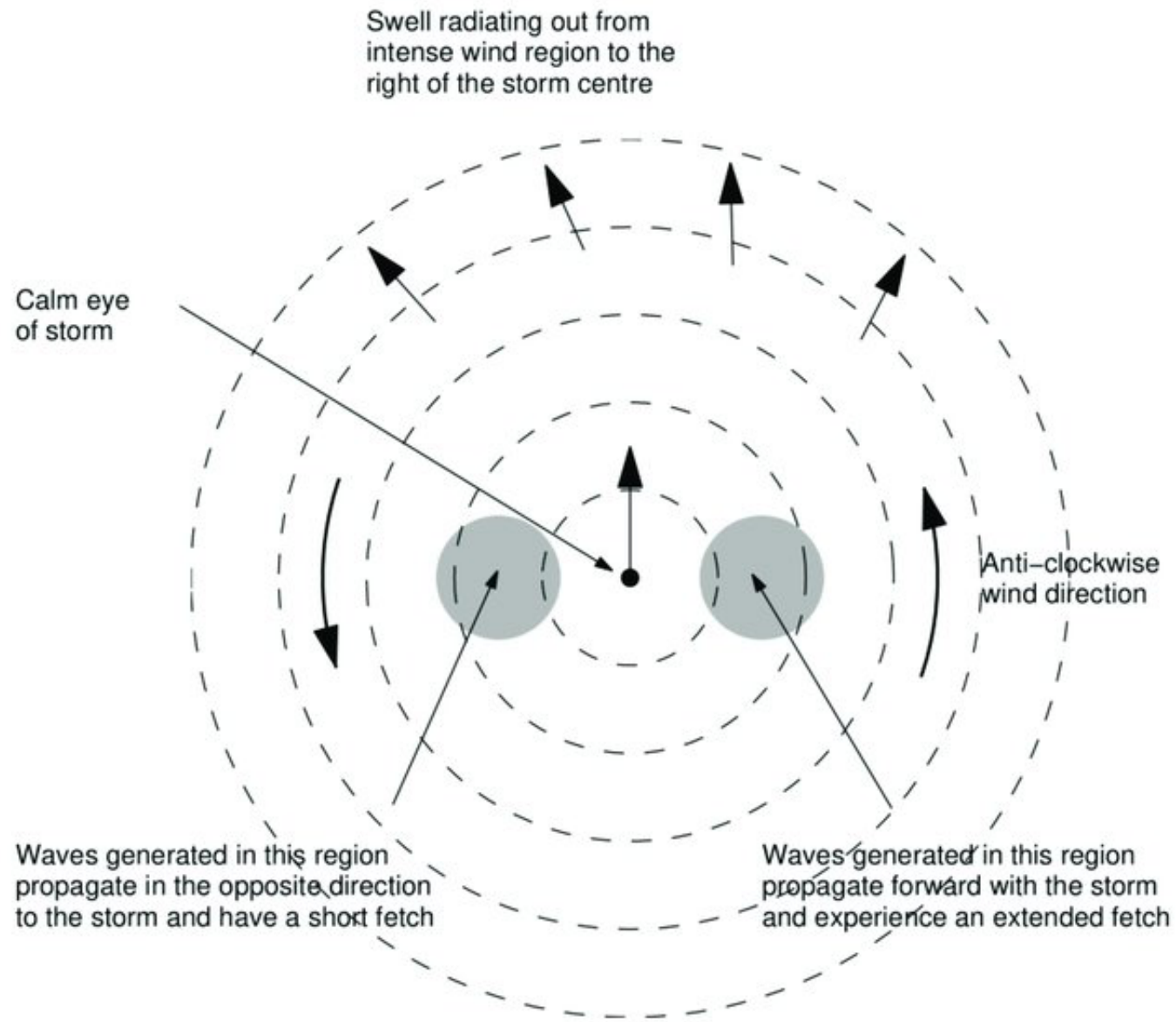
Wind & Wave Height



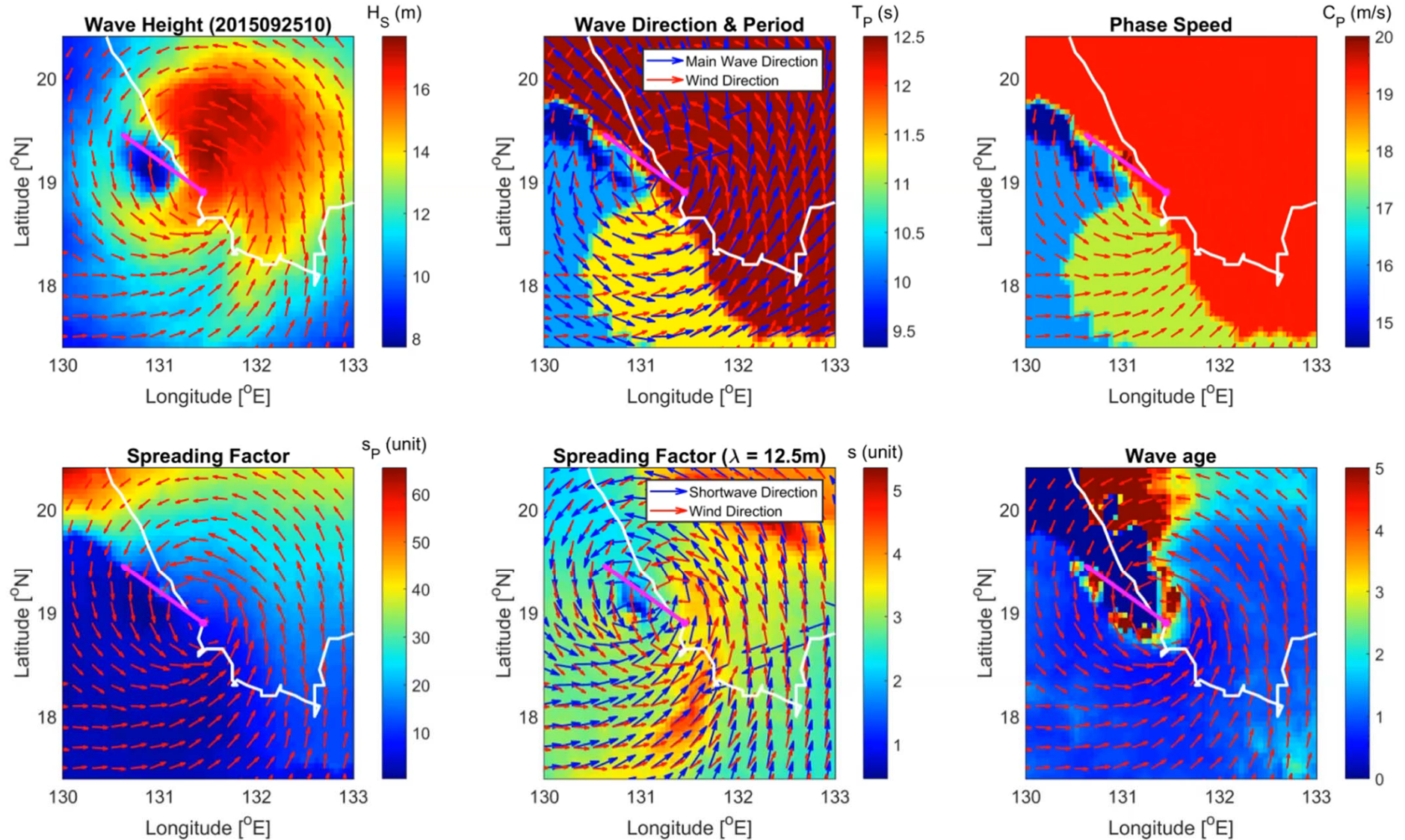
Typical Directional Spectra at 50 km radius of typhoon eye

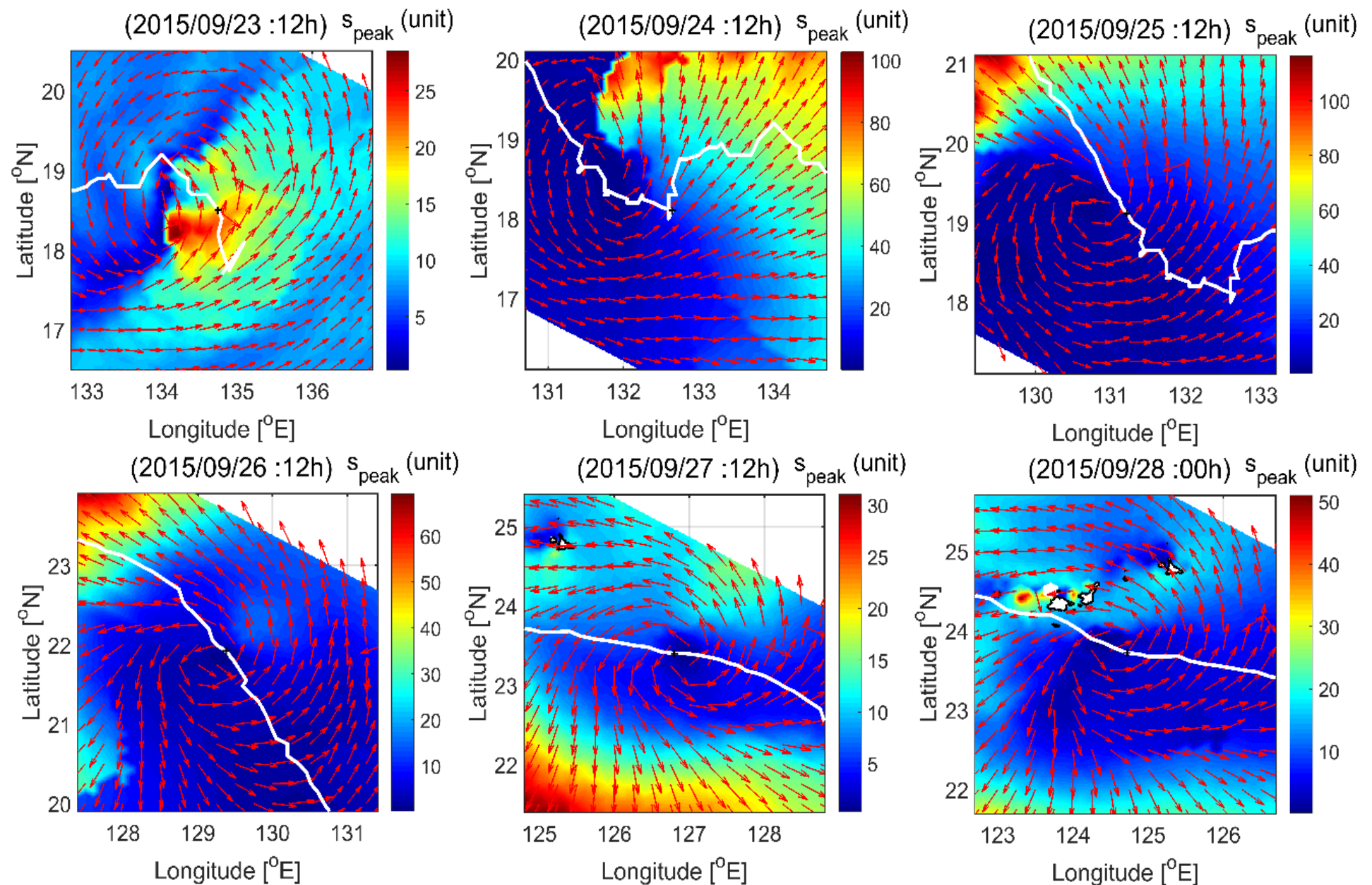


Narrower on RHS, wider and multi-peak on LHS



Wave height, Main Direction, Period, Spreading, Wave age near the typhoon eye

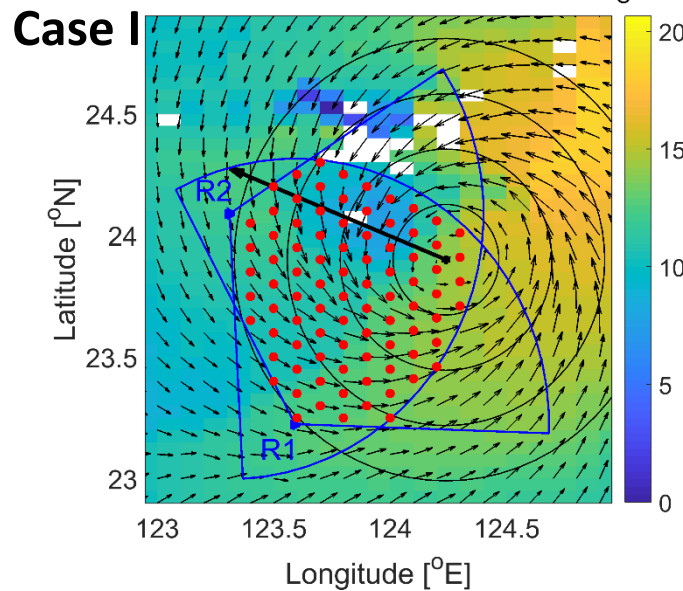




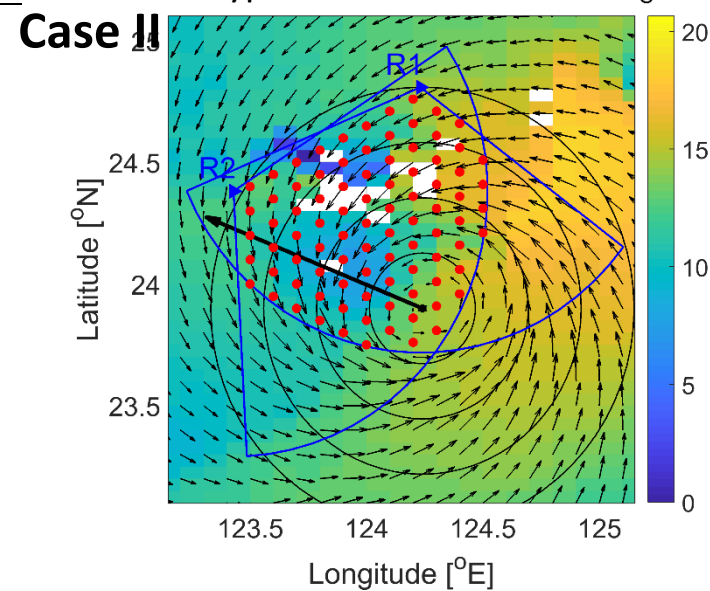
Spatial distribution of the main wave direction (red arrow) and the value of directional spreading parameter (colormap) around the typhoon center (black point)

Design of the locations of virtual Radars

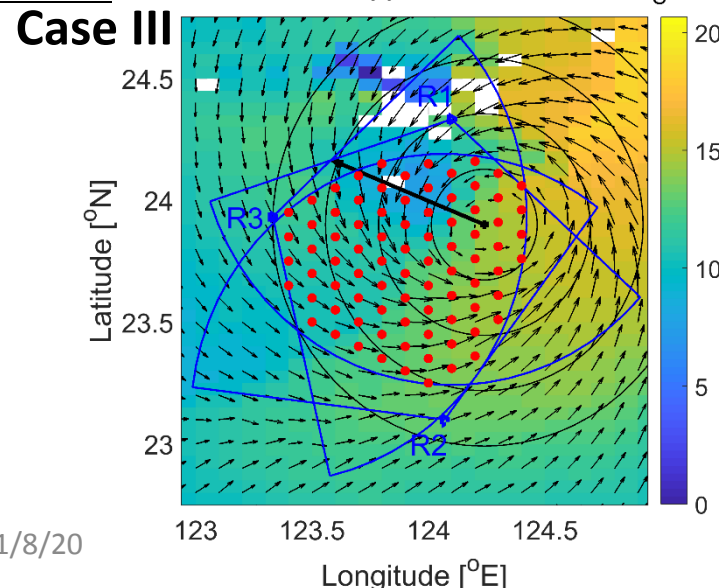
Two Radars for **LHS** of The Typhoon



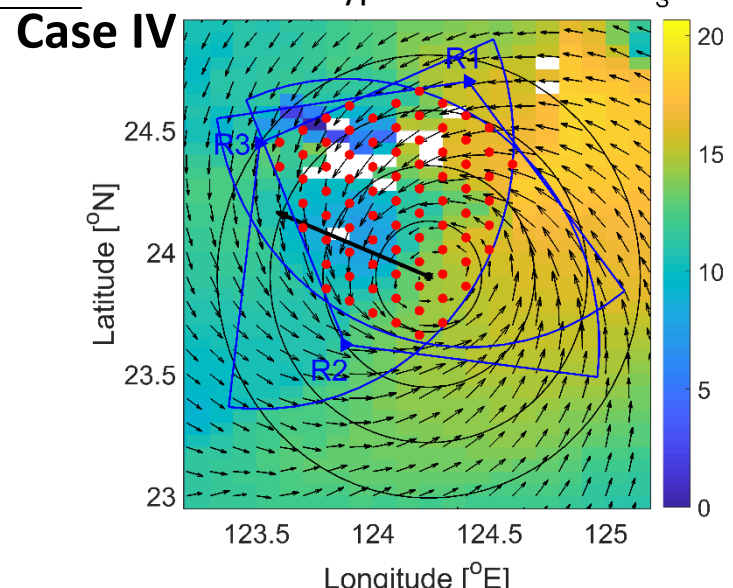
Two for **RHS** of The Typhoon



Three Radars for **LHS** of The Typhoon

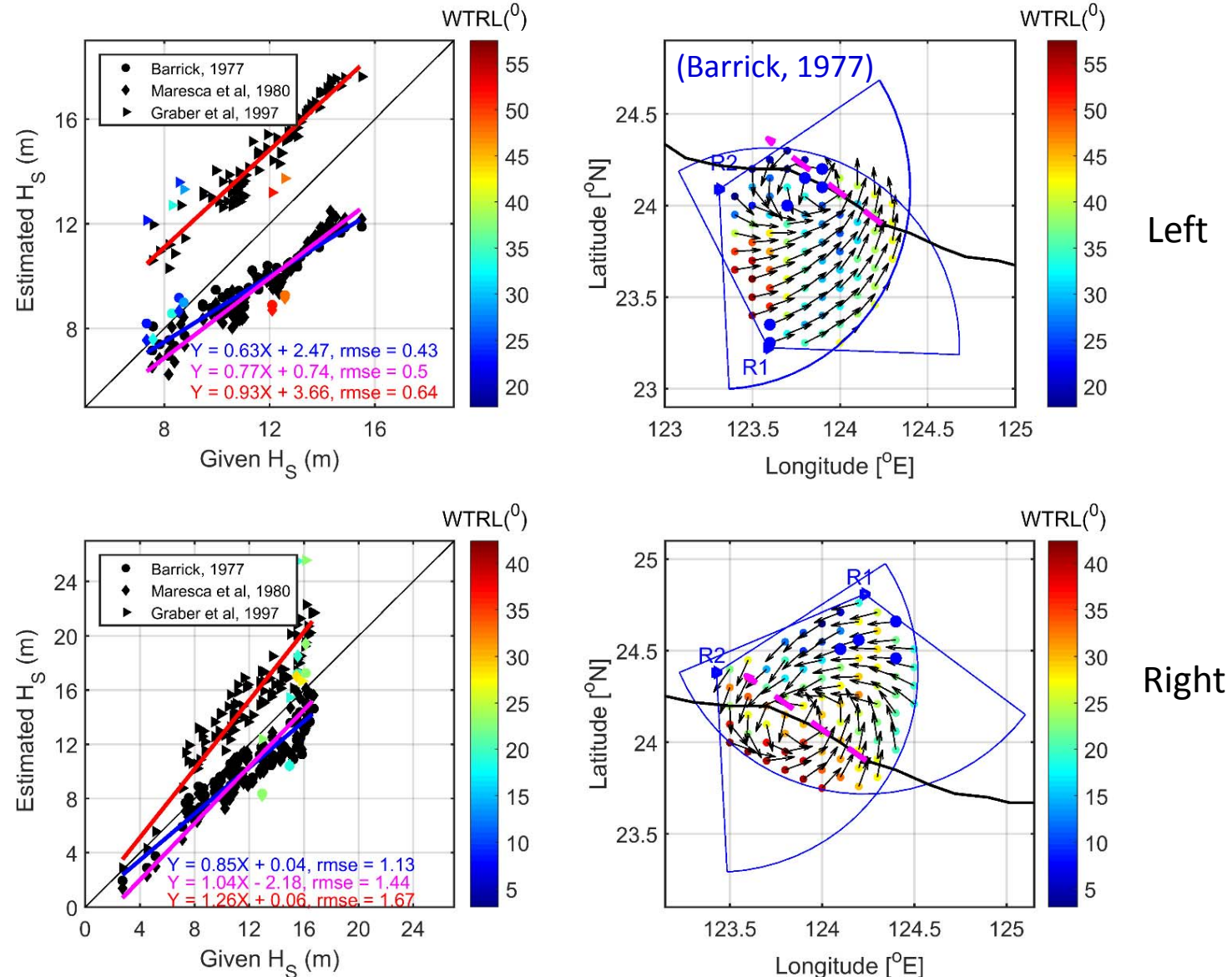


Three Radars for **RHS** of The Typhoon



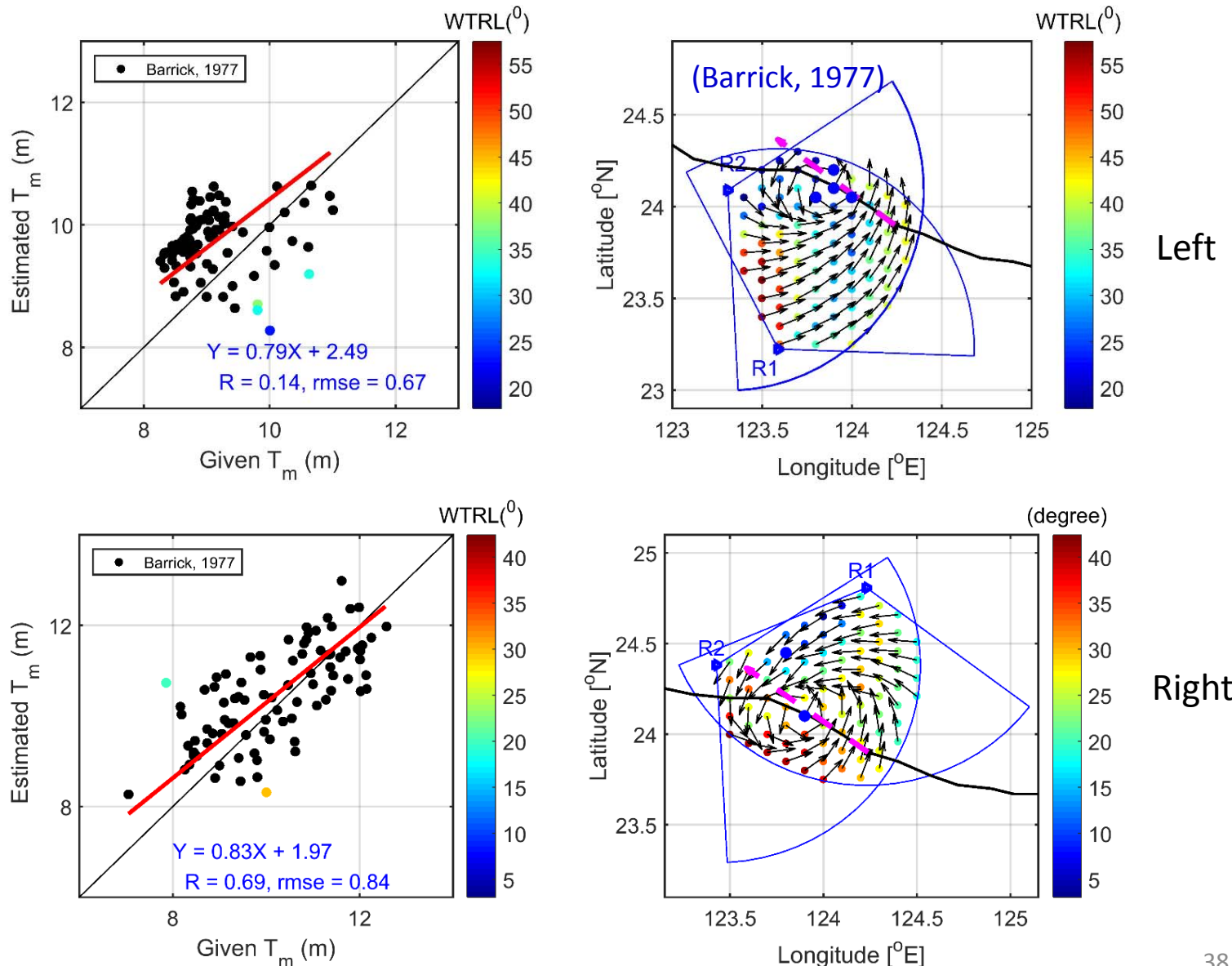
Lower uncertainty of Hs at Left Quadrants

(Sep 28, 2015: 03^h)



Lower uncertainty of Tm at Left Quadrants

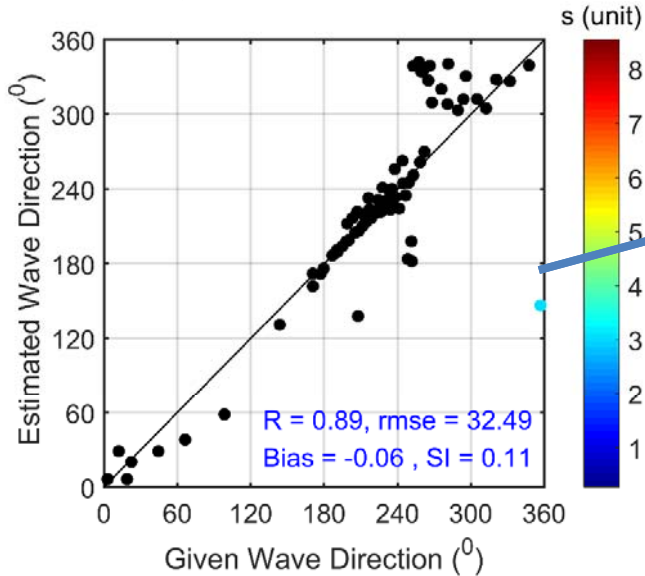
(Sep 28, 2015: 03^h)



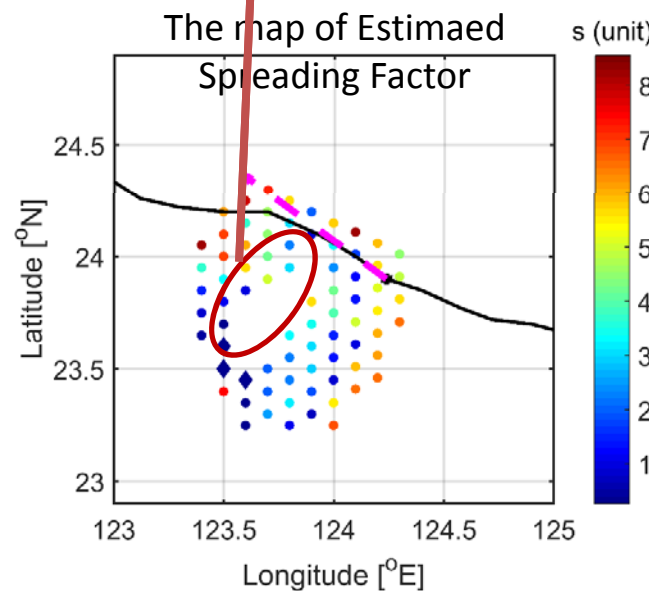
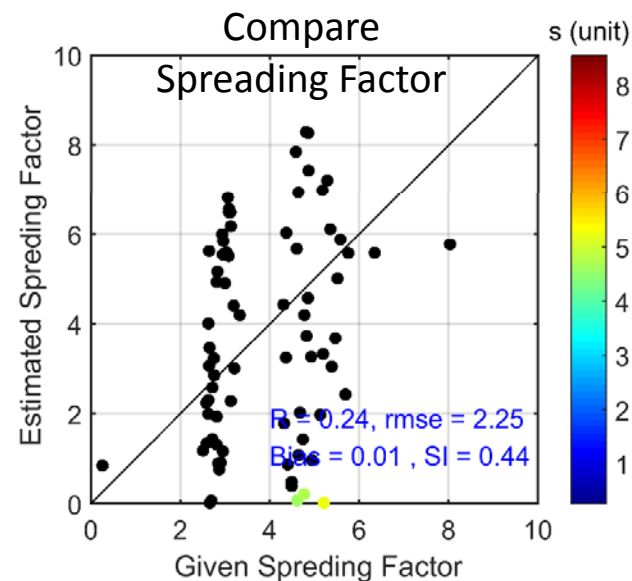
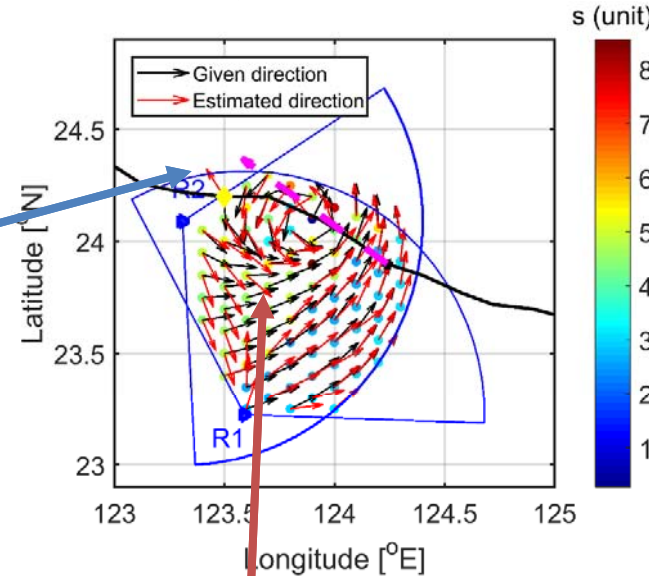
Directionality

(Sep 28, 2015: 03^h)

Compare Wave Direction



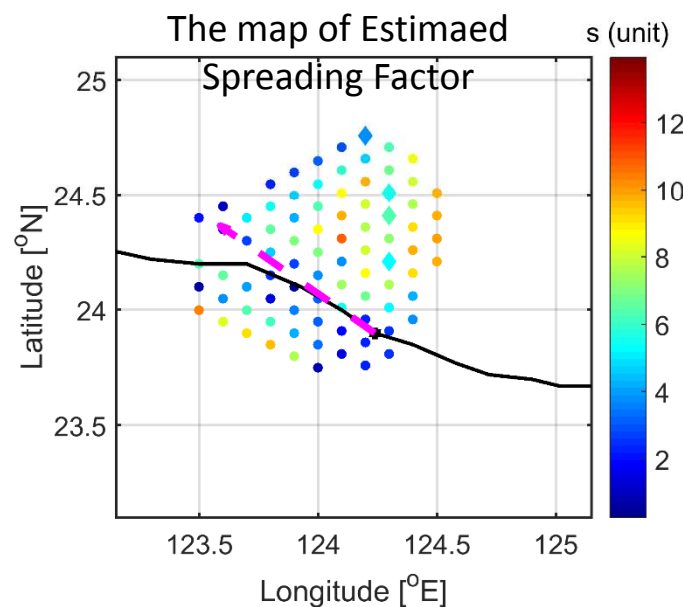
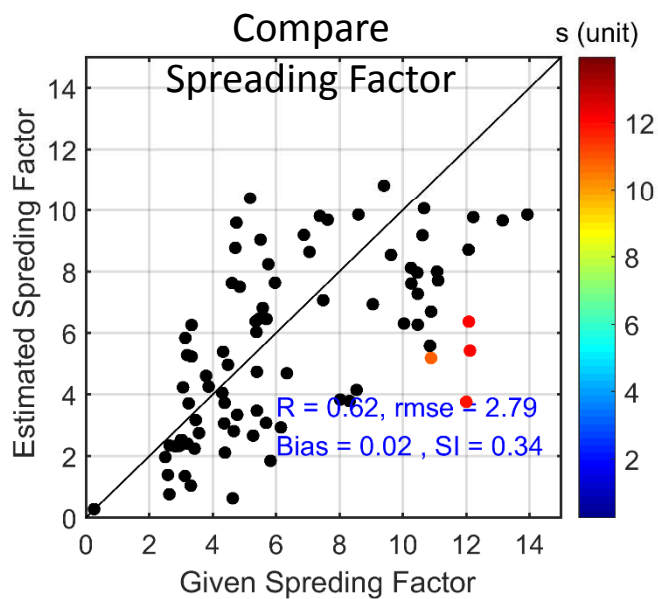
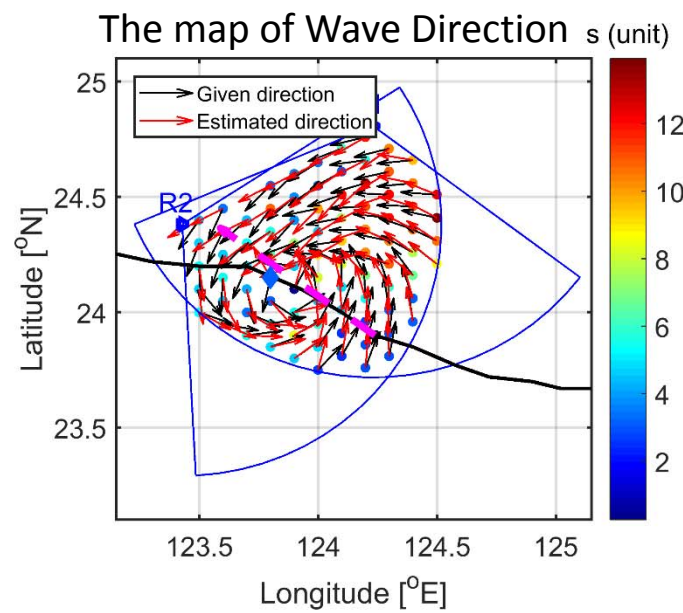
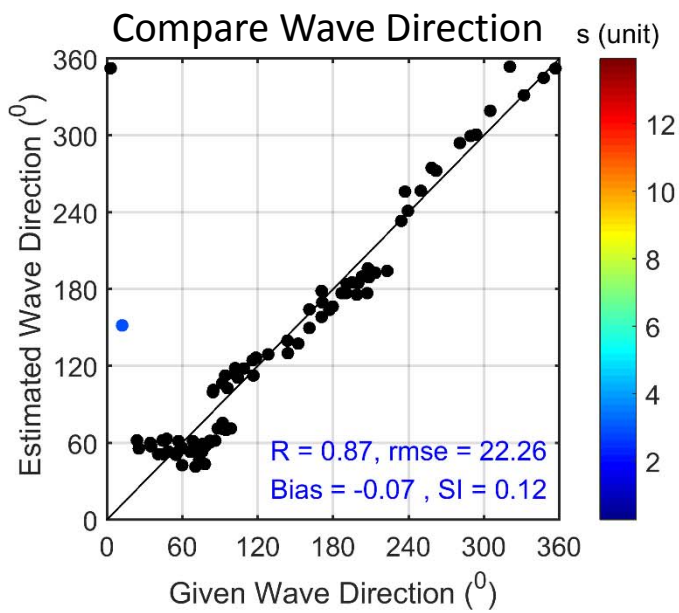
The map of Wave Direction



Concluding Remarks

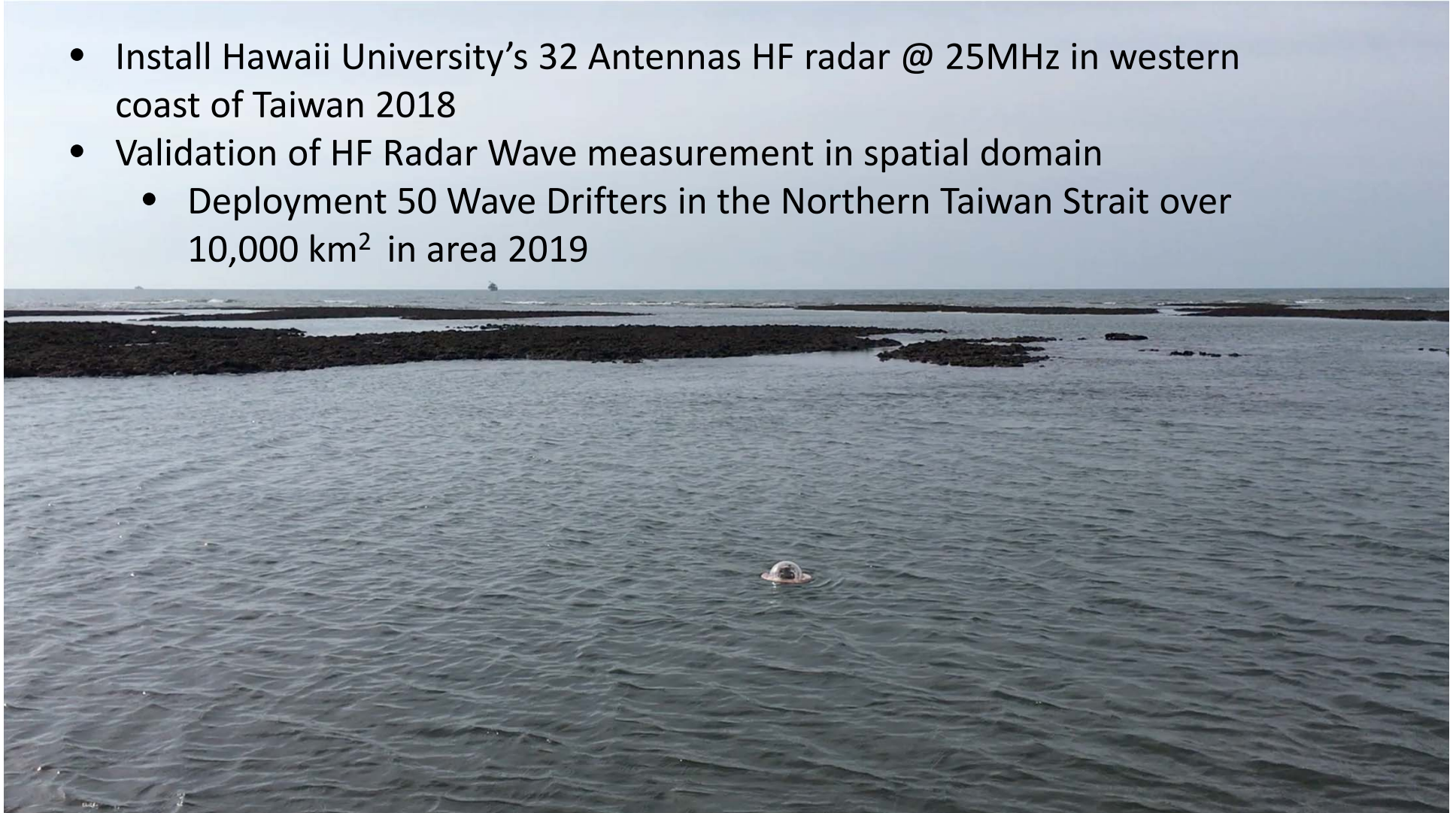
- The overall scatter index of H_s , which is defined as the RMSE normalized to the target value, is 22.7% for the monsoon case and 10% for the typhoon case; for T_m estimation, the overall SI is 9% for the monsoon case and 5% for the typhoon case.
- Both results show that the uncertainties of estimated parameters are reduced for the typhoon case compared with the monsoon.
- Slight differences exist between the SI values in the H_s estimations for the left-hand and right-hand quadrants. The SI is 7.6% for the left-hand-side quadrants, whereas the SI is 11% for the right-hand quadrants.

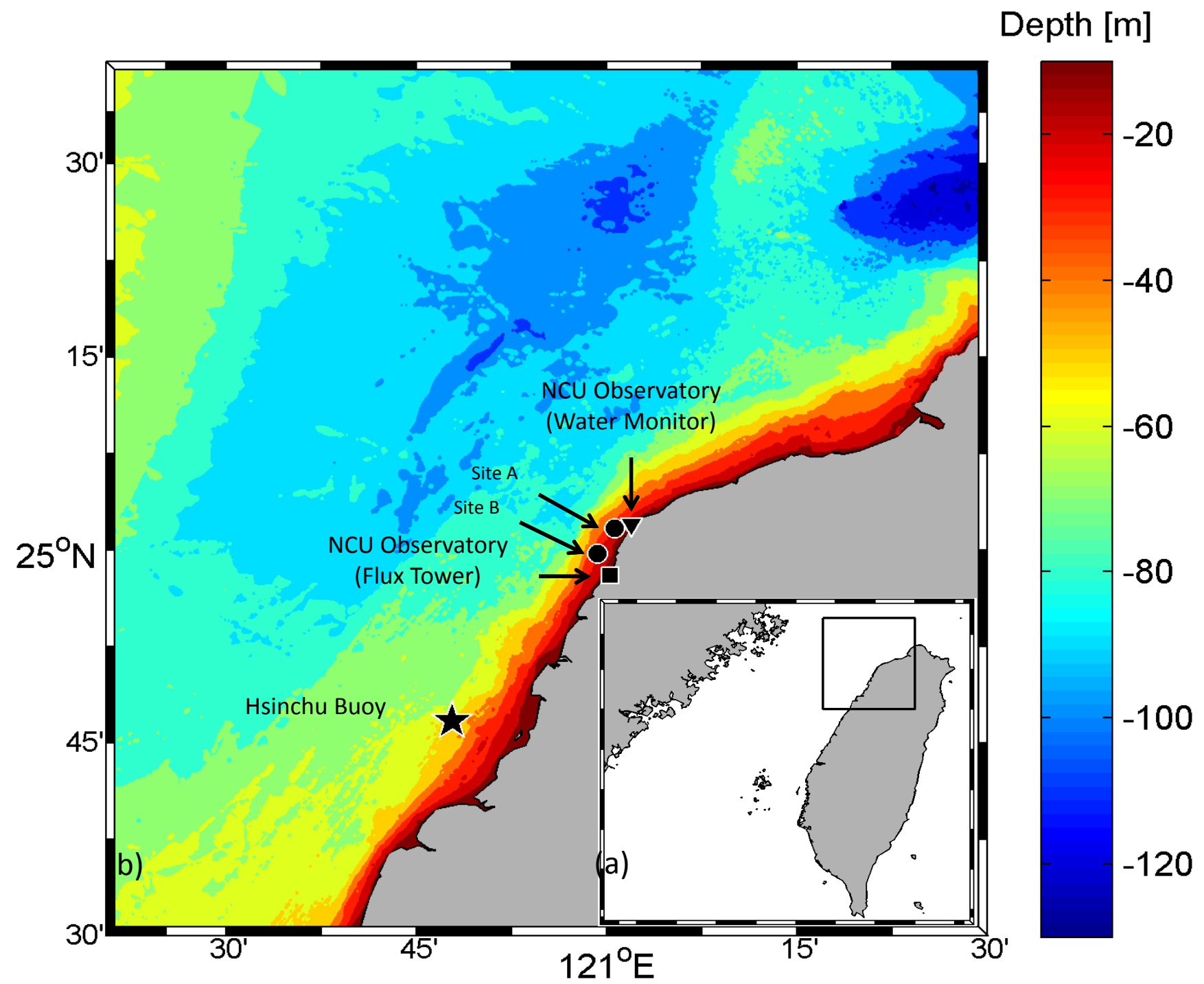
Comparing to Monsoon Cases, typhoon wave features greater directional spreading width for Bragg waves and thus benefit the performance of HF radar and the uncertainties are reduced.



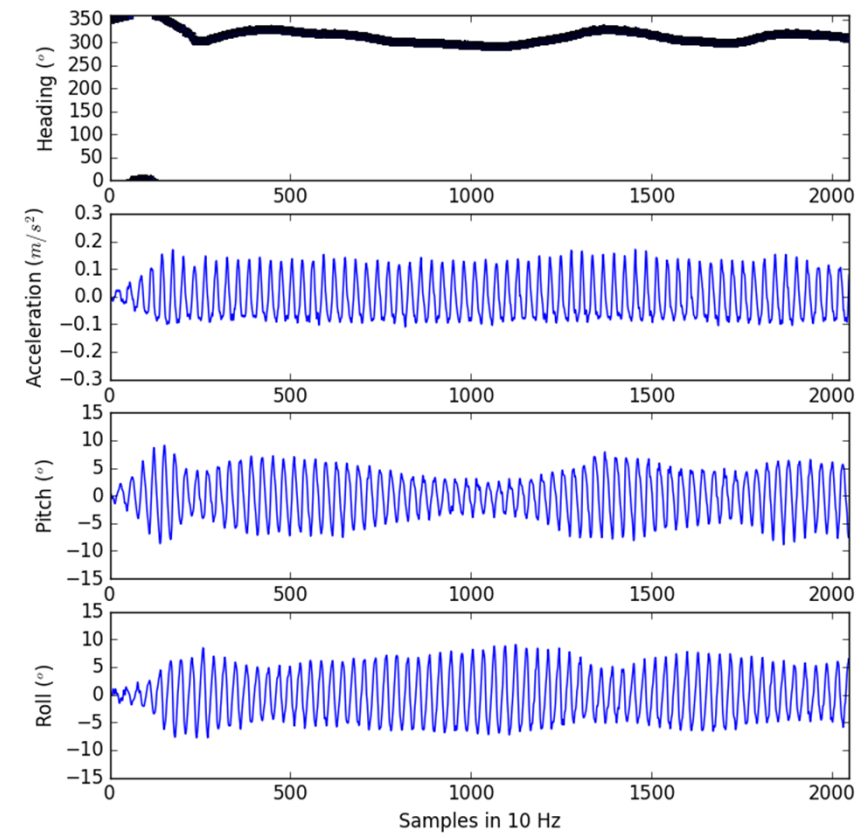
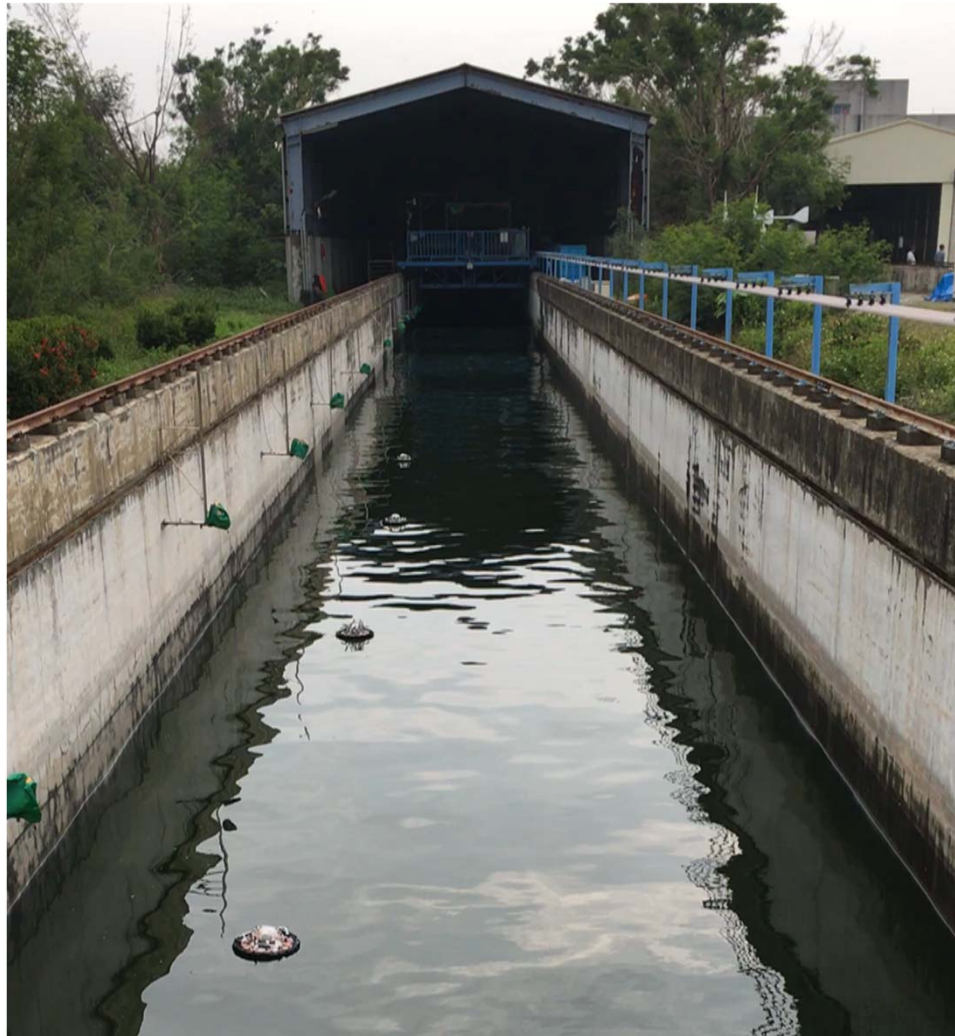
What's Next?

- Install Hawaii University's 32 Antennas HF radar @ 25MHz in western coast of Taiwan 2018
- Validation of HF Radar Wave measurement in spatial domain
 - Deployment 50 Wave Drifters in the Northern Taiwan Strait over 10,000 km² in area 2019



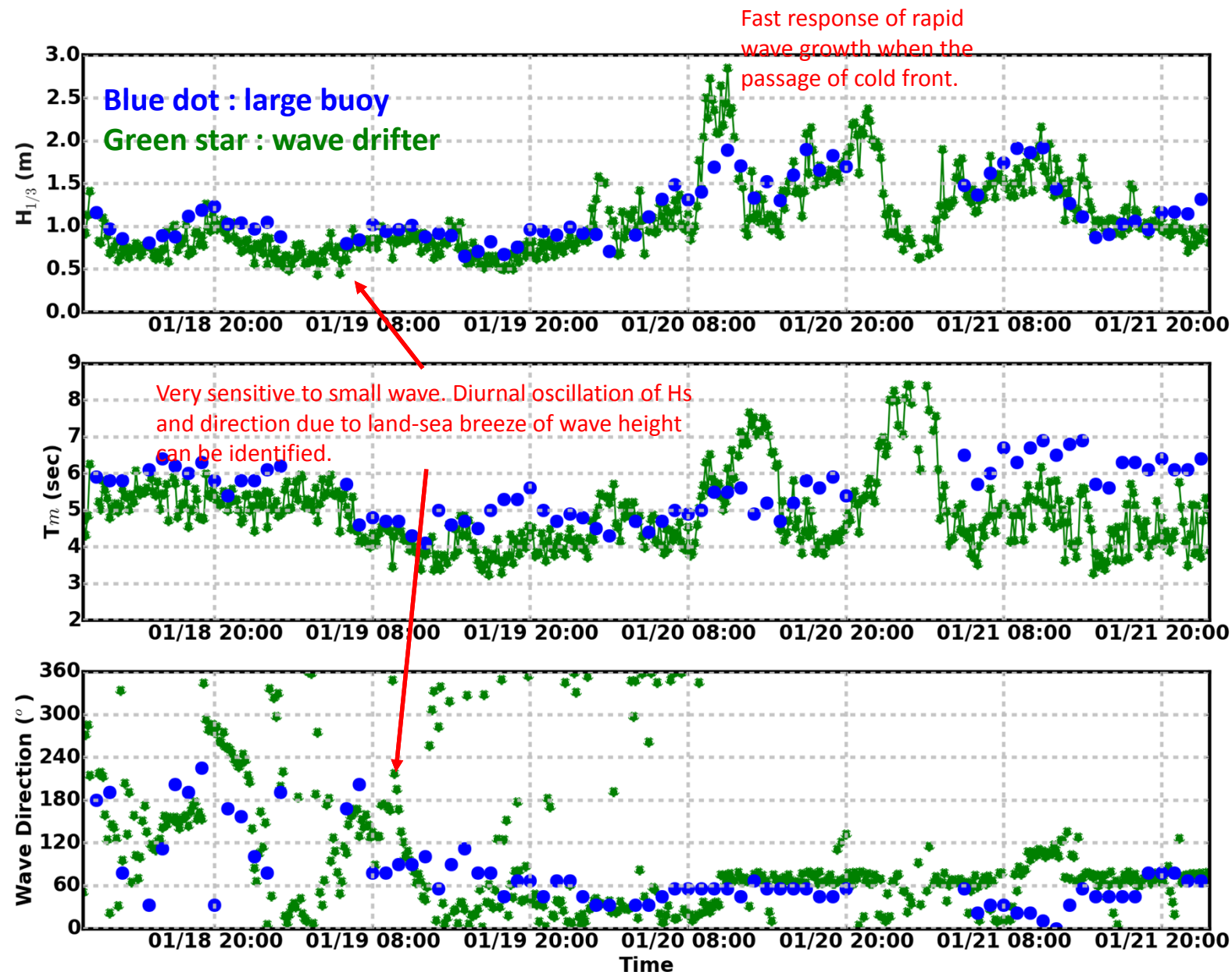


Wave Tank Calibration





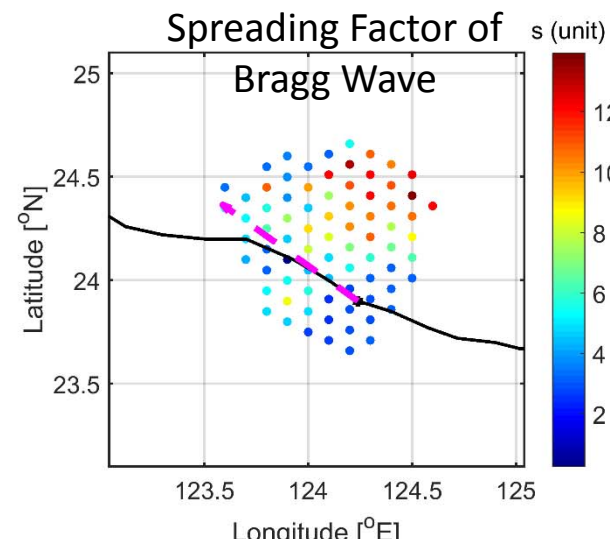
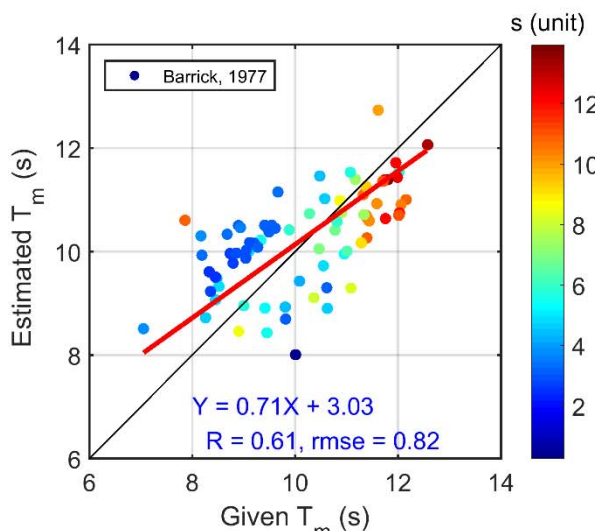
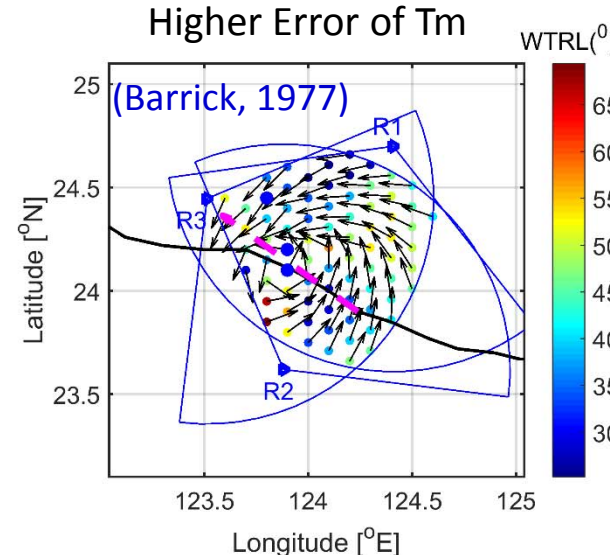
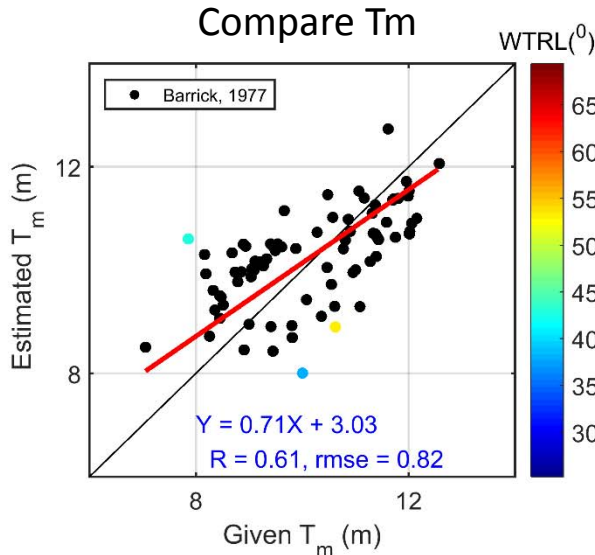
Comparisons with 2.5 Disc type Data Buoy



Where is the area of higher uncertainty of Tm?

Type IV radar constellation (Sep 28, 2015: 03^h)

Error > 10% Tm & Error > 2rmse



Where is the area of higher uncertainty of α_w ?

Type III radar constellation (Sep 28, 2015: 03^h)

